ANNUAL REVIEWS

Annual Review of Plant Biology

Structural Diversity in Eukaryotic Photosynthetic Light Harvesting

Masakazu Iwai,[1,2] Dhruv Patel-Tupper,[2] and Krishna K. Niyogi[1,2,3]

[1]Molecular Biophysics and Integrated Bioimaging Division, Lawrence Berkeley National Laboratory, Berkeley, California, USA; email: miwai@lbl.gov

[2]Department of Plant and Microbial Biology, University of California, Berkeley, California, USA

[3]Howard Hughes Medical Institute, University of California, Berkeley, California, USA

Annu. Rev. Plant Biol. 2024. 75:119–52

First published as a Review in Advance on February 15, 2024

The *Annual Review of Plant Biology* is online at plant.annualreviews.org

https://doi.org/10.1146/annurev-arplant-070623-015519

Keywords

cryo-EM, light-harvesting complex, LHC antenna organization, photoprotection, photosystem supercomplex, protein-protein interaction

Abstract

Photosynthesis has been using energy from sunlight to assimilate atmospheric CO_2 for at least 3.5 billion years. Through evolution and natural selection, photosynthetic organisms have flourished in almost all aquatic and terrestrial environments. This is partly due to the diversity of light-harvesting complex (LHC) proteins, which facilitate photosystem assembly, efficient excitation energy transfer, and photoprotection. Structural advances have provided angstrom-level structures of many of these proteins and have expanded our understanding of the pigments, lipids, and residues that drive LHC function. In this review, we compare and contrast recently observed cryo-electron microscopy structures across photosynthetic eukaryotes to identify structural motifs that underlie various light-harvesting strategies. We discuss subtle monomer changes that result in macroscale reorganization of LHC oligomers. Additionally, we find recurring patterns across diverse LHCs that may serve as evolutionary stepping stones for functional diversification. Advancing our understanding of LHC protein–environment interactions will improve our capacity to engineer more productive crops.

Contents

1. INTRODUCTION

Photosynthetic light harvesting is the process in which light energy is absorbed by pigment-binding antenna proteins and transferred to the reaction centers (RCs) of the two photosystems (PSI and PSII) to drive charge separation and photosynthetic electron transfer. The core structures of RCs are highly conserved in photosynthetic organisms. However, peripheral antenna systems, which funnel absorbed photon energy to RCs, are highly diverse, implying that different photosynthetic organisms have reshaped their light-harvesting antenna systems to optimize fitness in their natural habitats where light is often limiting (see the sidebar titled Different Types of Light-Harvesting Antenna Systems). The most abundant light-harvesting antenna system in nature, and thus the most impactful for global primary productivity, is composed of the light-harvesting complex (LHC) proteins in plants and most eukaryotic algae. LHC proteins direct the efficient transfer of absorbed light energy to nearby photosystems to achieve balanced excitation of PSI and PSII while also playing key roles in photoprotection to minimize photooxidative damage. A variety of LHCs exist even within a single species, highlighting adaptations necessary for efficient photosynthetic light harvesting under fluctuating light conditions.

Peripheral antenna systems: pigment-binding protein complexes surrounding photosystem core complexes involved in excitation energy transfer to the reaction centers

Light-harvesting complex (LHC): the term collectively used to indicate the family of eukaryotic light-harvesting complex proteins that bind chlorophylls and carotenoids

A growing database of DNA sequences from genomes and transcriptomes has provided insight into the evolution and diversification of LHCs, which has also aided in silico prediction of protein structures from amino acid sequences via algorithms such as AlphaFold (90). Revolutionary advancements in cryo-electron microscopy (cryo-EM) have also resolved in vitro protein–protein interactions between LHCs and photosystems at angstrom resolution. Furthermore, applying focused ion beam milling to cryo-electron tomography has opened new possibilities to visualize in vivo organization and assemblies of photosynthetic complexes under near-native conditions

DIFFERENT TYPES OF LIGHT-HARVESTING ANTENNA SYSTEMS

This review focuses on the three transmembrane light-harvesting complex (LHC) proteins in eukaryotic photosynthetic organisms. However, a variety of light-harvesting antenna systems are found in various photosynthetic organisms, such as those in the following list. Unique, undiscovered light-harvesting antenna systems could still exist in nature.

- Phycobilisomes are large, soluble, extrinsic membrane antenna complexes found in cyanobacteria and rhodophytes. The hemidiscoidal type is widely studied and usually contains phycoerythrin, phycocyanin, and allophycocyanin (53).
- Light-harvesting 1 (LH1) and LH2 complexes are the transmembrane antenna complexes found in purple photosynthetic bacteria. LH1 directly surrounds the reaction center (RC), and LH2 surrounds the LH1-RC complex (118).
- Chlorosomes are large antenna complexes found in low light-adapted anoxygenic phototrophic bacteria that contain up to 200,000 bacteriochlorophylls. The chlorosome is attached to the cytoplasmic side of the cell membrane through either baseplate complexes or Fenna–Matthews–Olson (FMO) proteins (211).
- Chlorophyll (Chl)-binding proteins (CBPs) found in cyanobacterial species have six transmembrane helices, bind different types of Chls (e.g., Chl *a*, Chl *b*, Chl *d*, divinyl-Chl *a*, and divinyl-Chl *b*), and function as a light-harvesting antenna system (174).
- Peridinin-chlorophyll proteins (PCPs) are water-soluble antenna proteins found in dinoflagellates (76).
- Cryptophyte phycobiliproteins (PBPs) share high sequence similarity with the αβ protomers of rhodophyte PBPs but exist as individual αβ dimers without forming into phycobilisomes (156). Both PCPs and PBPs exist in the thylakoid lumen and transfer absorbed energy to LHC proteins in the thylakoid membrane.

(208, 219). The confluence of these approaches provides exciting avenues to resolve molecular-level interactions in model systems and leverage phylogenetic sequence diversity to place those discoveries within the context of the photosynthetic tree of life.

Based on available structural evidence, this review focuses on the structural diversity of LHC proteins, the oligomeric interactions of LHCs, and the protein–protein interactions and assembly of LHCs with photosystems. We consolidate structural variation across several eukaryotes, emphasizing unique and shared light-harvesting strategies and the molecular interactions that make them possible. The rich diversity of LHC sequences and structures has the potential to accelerate in silico analyses and bioengineering of light-harvesting efficiency.

2. STRUCTURE AND DIVERSITY OF THE LHC SUPERFAMILY

2.1. The Structural Background of LHC Proteins

Eukaryotic LHC proteins are encoded entirely in the nuclear genome but localize exclusively to the chloroplast; thus, they are key contributors to plastid–host coevolution after ancestral endosymbiosis. Newly translated precursor LHC proteins contain a cleavable transit peptide sequence that directs them to the chloroplast, where they are then targeted to thylakoid membranes. Mature LHC proteins contain seven basic domains: three α-helical transmembrane (TM) domains (A, B, and C), stromal and lumenal loop domains, and N- and C-terminal domains whose amino acid sequence and structure dictate specific chlorophyll (Chl)–protein, carotenoid (Car)–protein, and protein–protein interactions (**Figure 1**). This section focuses on the characterization of LHC proteins of PSII (LHCII), which have been extensively studied for half a century (194).

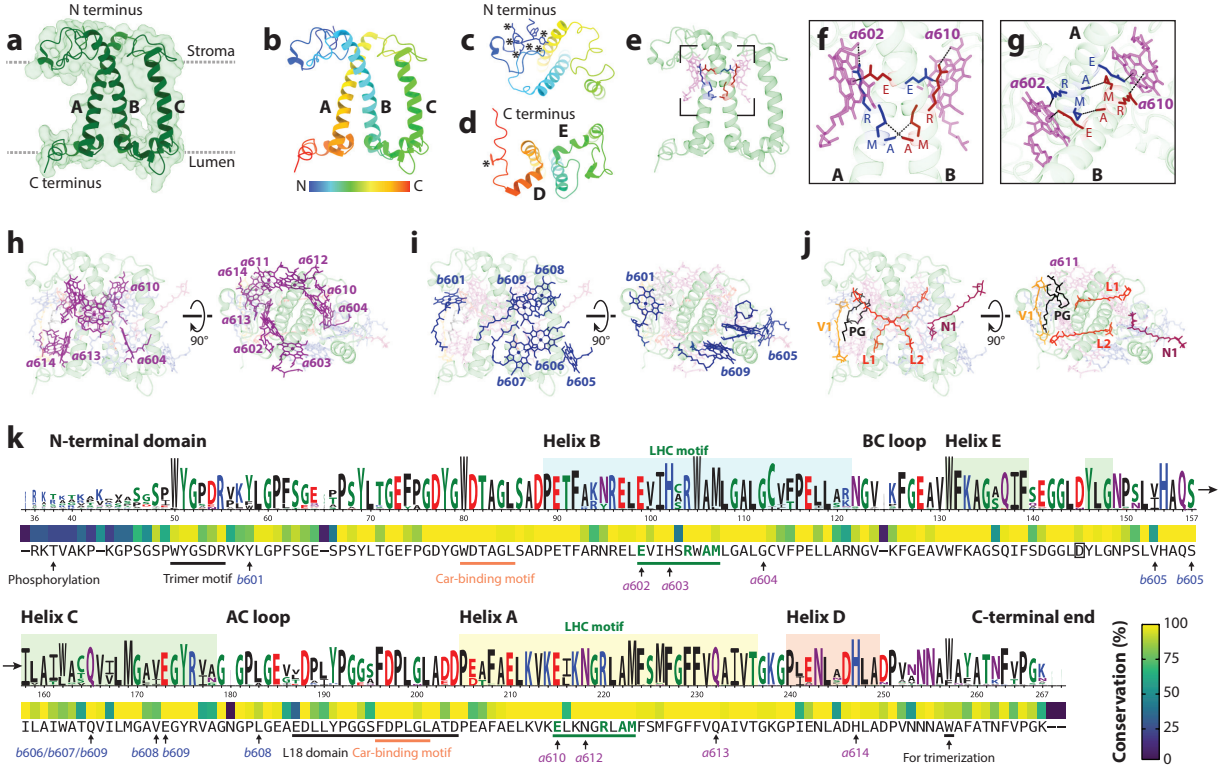

Figure 1

Structural aspects of LHC proteins. (*a*) A side-view protein structure of Lhcb1 from *Pisum sativum* (PDB ID 5XNL). The ribbon diagram, protein density, and an estimated thylakoid membrane boundary are shown. Helices A, B, and C are labeled. (*b*) The positions from N- and C-terminal ends are color coded. (*c*,*d*) The stromal and lumenal sides of Lhcb1 with the same color coding as in panel *b*. Amphipathic helices D and E are labeled. Asterisks indicate the trimer motifs at the N- and C-terminal regions. (*e*) The LHC motifs (E-X-X-X-X-R-X-A-M; X represents a non-conserved amino acid) at helices A and B with Chls *a*602 and *a*610 with close-up views from (*f*) the side and (*g*) the top (stromal side) are shown. The location of (*h*) Chls *a*, (*i*) Chls *b*, and (*j*) Cars are shown in side and top (stromal side) views. An alternative Chl nomenclature from Reference 180 corresponds to Chl 1 (*a*610), Chl 2 (*a*612), Chl 3 (*a*613), Chl 4 (*a*602), Chl 5 (*a*603), Chl 6 (*a*604), Chl 7 (*a*611), Chl 8 (*a*614), Chl 9 (*b*601), Chl 10 (*b*607), Chl 11 (*b*608), Chl 12 (*b*609), Chl 13 (*b*606), and Chl 14 (*b*605). (*k*) The sequence conservation of Lhcb1 in Viridiplantae. The color scheme for 1-letter amino acid codes is according to chemical properties: green for polar (G, S, T, Y, C), purple for neutral (Q, N), blue for basic (K, R, H), red for acidic (D, E), and black for hydrophobic (A, V, L, I, P, W, F, M). The heat map for conservation (%) is indicated. The protein sequence of *Arabidopsis thaliana* Lhcb1.3 is shown below the heat map as a reference. *a*611 is not indicated because it binds to PG (as shown in panel *j*). A possible protonatable aspartate residue is indicated in a box (D145). Helices are indicated as boxes with the same color code used in panel *b*. The sequence of Lhcb1 homologs from the following species are used for the sequence conservation analysis (UniProt identifiers are indicated within parentheses): *Arabidopsis thaliana* (P04778), *Chenopodium quinoa* (A0A803KS73), *Kalanchoe fedtschenkoi* (A0A7N0U2A0), *Vitis vinifera* (A5C4U9), *Gossypium mustelinum* (A0A5D2Z8K8), *Spinacia oleracea* (P12333), *Capsicum baccatum* (A0A2G2W7Q4), *Handroanthus impetiginosus* (A0A2G9I1G2), *Camellia sinensis* (A0A4S4EZG3), *Nicotiana attenuata* (A0A314LFJ8), *Phaseolus angularis* (A0A0L9VKL9), *Thalictrum thalictroides* (A0A7J6VVP0), *Cinnamomum micranthum* (A0A3S3NIV5), *Ensete ventricosum* (A0A444FZZ6), *Zea mays* (P12329), *Sorghum bicolor* (C5X7M3), *Triticum aestivum* (A0A3B6N1F1), *Oryza sativa* (P12331), *Elaeis guineensis* (A0A6I9RCC8), *Amborella trichopoda* (U5D860), *Pinus sylvestris* (P15193), *Pinus thunbergii* (P10049), *Polystichum munitum* (P15195), *Selaginella moellendorffii* (D8QN27), *Physcomitrium patens* (Q9SXW8), *Marchantia polymorpha* (A0A2R6W0R6), *Chara braunii* (A0A388KXN5), *Klebsormidium nitens* (A0A1Y1ITA5), *Chlamydomonas reinhardtii* (Q93VE0), *Volvox carteri* (D8TZW8), *Haematococcus lacustris* (A0A6A0AA98), *Chlorella variabilis* (E1ZJ10), *Tetradesmus obliquus* (A0A383WFN3), *Auxenochlorella protothecoides* (A0A087SFH6), and *Ostreococcus tauri* (A0A090M5W1). Abbreviations: Car, carotenoid; Chl, chlorophyll; LHC, light-harvesting complex; PDB ID, Protein Data Bank identifier; PG, phosphatidylglycerol. Panels *a–j* were created using UCSF ChimeraX (124). Panel *k* was created using WebLogo (38, 166).

2.1.1. The transmembrane helices. The three TM helices comprise the most evolutionarily conserved domain among different LHCs, and they form the core LHC structure that contains pigments and lipids at specific locations (120). Helices A and B have twofold symmetry, spanning the membrane plane diagonally. These helices have sequence similarity of 40–50%, depending on the species, and may have originated through an internal gene duplication. Both helices contain an LHC motif (E-X-X-X-X-R-X-A-M), in which the glutamate in helix B and the arginine in helix A coordinate a Chl *a* (*a*602), and the glutamate in helix A and the arginine in helix B coordinate another Chl *a* (*a*610) (**Figure 1*e–g***). These glutamate-arginine pairs are important for protein folding and stabilization (11). Helix C is about two-thirds shorter in length than helices A and B and spans the membrane vertically. Helix C is the second helix in the protein, connecting to helices B and A through the lumenal and stromal loops, respectively (**Figure 1*b–d***). The sequence of helix C is more variable among different species than the other helices, with functional consequences in protein–protein interactions.

2.1.2. The lumenal loop. The lumenal loop region that connects helices B and C (BC loop) is more flexible than the three TM domains (51). This BC loop contains an amphipathic helix E (**Figure 1*d***). The overall flexibility of the BC loop is caused by the domain between helices E and C (60), in which a well-conserved aspartate residue may play a photoprotective role via protonation-induced conformational changes upon lumenal acidification in high light (HL) (14). BC loops across the LHC superfamily show structural variation, suggesting functional diversity within these regions.

2.1.3. The stromal loop. Similar to the lumenal loop, the stromal loop that connects helices A and C is also more structurally flexible than the main body of LHCs (180) (**Figure 1*c***). This loop region contains the well-conserved L18 motif, which, together with helix A, is bound by chloroplast signal recognition particles for posttranslational targeting of imported LHC proteins to thylakoid membranes (181). The AC loop and the stromal side of helix A also contain multiple well-conserved negatively charged residues that, alongside the positively charged N-terminal domain, generate a distinct surface charge distribution that may play a role in interactions between different thylakoid membrane surfaces (180).

2.1.4. The N-terminal domain. The N-terminal domain is exposed to the stromal side of thylakoid membranes and is the least conserved domain within LHCs (**Figure 1*c*,*k***). This domain is the most flexible region within LHCs but is structurally confined to a narrow area above helices A and B (51, 60). This structural flexibility is suggested to mediate a photoprotective switch via conformational changes around specific Chls (*a*611 and *a*612) (115) (**Figure 1*b*,*i*,*k***). The N-terminal domain contains multiple serine and threonine residues that can be phosphorylated, which influences the redistribution of excitation energy between the two photosystems via state transitions (197). Phosphorylation of a well-conserved threonine residue in the N-terminal domain mediates protein–protein interaction with PSI (142, 143). Additionally, phosphorylation disrupts the overall positive surface charge of the protein, which could affect additional protein–protein and intermembrane interactions (180). The N-terminal domain can also contain a trimer motif (**Figure 1*c***), which mediates trimerization of some LHC proteins (75).

2.1.5. The C-terminal domain. The C-terminal domain is generally conserved but varies in its length among different LHC proteins. There is an amphipathic helix D (**Figure 1*d***), which contains a well-conserved Chl-binding site (*a*614). Helix D is thought to undergo conformational changes through protonation of its carboxylate groups upon lumenal acidification in HL, which might have a photoprotective role through nearby Chls and Cars (45). This helix is also important for protein–protein interactions. Toward the C-terminal end, there is another short amphipathic

Lumenal acidification: build-up of protons in the thylakoid lumen from electron transport and constrained proton efflux via ATP synthase due to limited P_i

State transitions: the redistribution of excitation energy transfer between PSI and PSII by reversible phosphorylation of LHCII

helix in which a tryptophan residue stabilizes the trimeric state of some LHC proteins (107) (**Figure 1*d***).

Soret band: one of the two major peaks in the absorption spectrum of Chl at shorter than 500 nm; also called B band and further classified into B_x and B_y

Q band: one of the two major peaks in the absorption spectrum of Chl at longer than 500 nm; further classified into Q_x and Q_y

Triplet excited state: a longer-lived (~millisecond order) Chl state formed by intersystem crossing and capable of generating $^1O_2$

2.2. Diversities of Pigment Binding in LHC Proteins

Folding of LHC proteins requires Chls and Cars (11), but the in vivo assembly mechanisms are still unclear (see 39 for a review). Varied Chl/Car pigment compositions in different LHCs affect their capacity for energy transfer, structural integrity, and photoprotection. For example, there are 14 Chls (8 Chl *a* and 6 Chl *b*) in the monomeric form of the Lhcb1 protein (**Figure 1*b*,*i*,*k***). These Chl-binding sites in LHCs are well-conserved across Viridiplantae (green lineage), suggesting that their location and orientation are fine-tuned for ultrafast energy transfer without creating unwanted quenching sites (167). Although Chl-binding specificity can be modified in vivo (74), the spatial availability of Chl surrounding the binding sites, site selectivity, and protein-folding dynamics largely determine binding affinity to Chl *a* or Chl *b* (55, 141).

The LHC proteins in cryptophytes, dinoflagellates, haptophytes, and stramenopiles replace Chl *b* with Chl *c*, whose Soret band absorption is considerably larger, and Q band absorption is small and blueshifted (19). Therefore, Chl *a*/*c*–binding proteins [e.g., fucoxanthin-Chl proteins (FCPs)] have the ability to absorb blue-green light efficiently and promote fitness in aqueous environments with poor red light penetrance. Interestingly, Chl *c* can undergo protonation at its acrylate group, which causes an approximately 25-nm redshift of light absorption and may affect excitation energy dynamics upon lumenal acidification in HL (199).

Chl *d*, which has a redshifted Q_y band absorption, can replace Chl *a* and function in phycobiliproteins in cyanobacteria (215). Although no eukaryotic LHC proteins binding Chl *d* have been found in nature, a recent in vitro reconstitution study demonstrated that Chl *d* can functionally replace Chl *a* in plant LHC proteins, conferring strong absorption in far-red light (56). This could pave the way to engineering plant LHC proteins with improved light absorption at far-red wavelengths, even possibly with Chl *f*, which has the most redshifted light absorption among all Chl species (30). Intriguingly, the Antarctic chlorophyte *Prasiola crispa* has evolved a ring-shaped structure composed of 11 LHC proteins that exhibits a large far-red absorption band at approximately 707 nm in the absence of Chl *d* or Chl *f* (98), suggesting that structural differences may also be sufficient to expand absorption spectra and ecological niches.

In addition to 14 Chls, 4 Car-binding sites are designated in the monomeric form of the Lhcb1 protein of plants: L1, L2, N1, and V1 (**Figure 1*j***). The specific Car-binding motifs are located in the stromal N-terminal and AC loop domains immediately preceding helices A and B (11) (**Figure 1*k***). Unlike Chl molecules, whose stable binding is caused by the hydrogen bonding between the central magnesium in the chlorin ring and amino acid side chains (or water bound to a main chain carbonyl), the binding of Cars is mainly stabilized through van der Waals interactions with nearby Chl molecules (123). The Car occupancy at the L1 site is the most important for stabilizing the protein structure (11) and quenching the triplet excited state of Chls (2, 25). Both L1 and L2 sites can be occupied by lutein, violaxanthin, or zeaxanthin (61), where all Cars are sufficient for quenching of triplet Chls (25, 164). Car binding at the N1 site is not required for protein folding when lutein, violaxanthin, and/or zeaxanthin exist in the L1 and L2 sites (61). The N1 site is normally occupied by neoxanthin, which can scavenge superoxide anions, but violaxanthin can also bind there when neoxanthin is missing (41). Violaxanthin and lutein can bind to the V1 site, but they cannot transfer excitation energy to Chls, unlike Cars in L1, L2, and N1 sites (22, 37). Also, the Car binding at the V1 site is weak, so it is considered to be the site for the photoprotective Car zeaxanthin, which is generated from violaxanthin upon lumenal acidification in HL (213). Car-binding sites can be occupied by different Cars in different LHCs, such as β-carotene at the

N1 site in LHCs of PSI (LHCIs) (154) or siphonaxanthin/siphonein at the L1/L2 sites in LHCs of some marine chlorophytes (169), showcasing the pigment-binding flexibility of LHC structures.

The LHC proteins in Chl *c*–containing algae have different Car compositions, such as alloxanthin, crocoxanthin, diadinoxanthin, diatoxanthin, fucoxanthin, monadoxanthin, peridinin, vaucheriaxanthin, and possibly other Cars, depending on the species (19, 212, 223). Structural advances, such as the recently observed 1.8-Å crystal structure of FCP, have been critical in understanding how divergent pigment types and compositions can maintain highly efficient energy transfer in contrasting light environments (203).

2.3. Thylakoid Lipids in LHC Proteins

All LHC proteins are located in the thylakoid membrane, which is one of the most complicated membrane systems in nature. The thylakoid membrane contains ~80% uncharged glycolipids [~50% monogalactosyldiacylglycerol (MGDG) and ~30% digalactosyldiacylglycerol (DGDG)] and ~20% negatively charged lipids [~10% sulfoquinovosyldiacylglycerol (SQDG) and ~10% phosphatidylglycerol (PG)] (218). MGDG is a nonbilayer lipid, but it forms a lamellar phase by stabilizing the trimer formation of LHCII in thylakoids (168, 176). While MGDG mediates an interaction between PSII and LHCII (226), DGDG stabilizes the one between PSI and LHCI (67). Despite being the least abundant lipid in thylakoids, the lack of PG causes severe defects in thylakoid development (68). PG is essential for LHCII trimerization as it is located at the interface between each of the monomers (120, 180) (**Figure 1*j***). Because purified protein complexes often lack full complements of lipids due to detergent solubilization, it is still unclear how thylakoid lipids are involved in the assembly of protein complexes.

2.4. Diversity of the LHC Superfamily

There is significant genetic diversity in LHC proteins across photosynthetic eukaryotes consisting of the green and red lineages. The green lineage, or Viridiplantae, includes prasinophytes, chlorophytes, streptophyte algae, and embryophytes (i.e., bryophytes, ferns, gymnosperms, and angiosperms). The red lineage comprises rhodophytes, cryptophytes, haptophytes, dinoflagellates, and stramenopiles (e.g., diatoms, brown algae, and eustigmatophytes). Genes within the LHC superfamily are identified based on an LHC sequence motif within characteristic TM domains (85). More divergent LHC relatives may not be involved directly in photosynthetic light harvesting, and they have different structural features around the LHC motif that enable them to perform novel functions. For example, ferrochelatase II forms a dimer that is stabilized by an LHC motif, which may fine-tune the catalytic activity of heme biosynthesis (178). Please see **Supplemental Table 1** for various LHC superfamily members found in photosynthetic eukaryotes (19, 50, 58, 106).

Supplemental Material >

2.4.1. High light-inducible protein. High light-inducible proteins (HLIPs) are single TM proteins first identified in cyanobacteria (52). In *Synechocystis*, HLIP heterodimers protect PSII assembly/repair intermediates from HL at different steps by serving as energy quenchers via bound Chls and Cars (31, 96, 97, 179) and may bind to a PSII assembly intermediate complex in the same way as the Psb34/Tsl0063 assembly factor (210, 220).

2.4.2. One-helix protein. One-helix proteins (OHPs) are HLIP orthologs found in photosynthetic eukaryotes (58). Similar to the HLIP heterodimer in cyanobacteria, OHPs play a critical role in the early steps of PSII assembly via association with a PSII assembly factor (71, 113) and also appear essential for plastid development (128). OHP1 and OHP2 form a heterodimer that binds Chls and Cars and may supply those pigments to PSII assembly intermediates and serve as an energy quencher during PSII assembly (72).

2.4.3. Stress-enhanced protein and light-harvesting-like protein 3. Stress-enhanced proteins (SEPs) are double-TM proteins that exist ubiquitously in photosynthetic eukaryotes (58). Among the four *Arabidopsis* SEP genes (*SEP1/LIL4*, *SEP2/LIL5*, *LIL3.1*, and *LIL3.2*), the *LIL3*s are the most studied, and the lack of both genes results in severe growth defects (193). Similar to OHPs, LIL3s form a homo- and heterodimer with the capacity to bind Chls (73). LIL3.1 forms a dimer and binds 4–6 Chls *a* and 2 zeaxanthins when heterologously expressed in *Synechocystis*, displaying an energy-quenching capability (177). LIL3 dimers interact with geranylgeranyl reductase and protochlorophyllide oxidoreductase and play an essential role in the later steps of chlorophyll biosynthesis (73, 192). The ancestral proteins of HLIPs/OHPs and SEPs are hypothesized to be the evolutionary origin of LHC proteins (52, 126).

2.4.4. Early light-inducible protein. Early light-inducible proteins (ELIPs) have only been found in the Viridiplantae (58), and their transcripts and proteins appear transiently during deetiolation and disappear before chloroplast development is complete (66). ELIPs have 3 TM domains, the first and third helices of which contain LHC motifs similar to helices A and B of LHCs. ELIP monomers can bind 4 to 5 Chls and 2 luteins (177). It has been suggested that ELIPs bind free Chls or modulate Chl synthesis to prevent the accumulation of free Chls (79, 200), function as energy quenchers (177), and/or bind xanthophylls (104), though their functional roles during early stage chloroplast development remain unclear (79, 159).

An ELIP-like protein, maintenance factor for PSI (MSF1), accumulates and stabilizes PSI machinery under heat shock and iron/copper limitation but not HL in the chlorophyte *Chlamydomonas* (222). Another ELIP-like protein, carotenoid biosynthesis-related protein (CBR), overaccumulates in the desert chlorophyte *Chlorella ohadii* under extremely HL and may play a unique role in photoprotection (108).

2.4.5. Prasinophyte-specific LHC protein. LHC proteins found in prasinophytes (LHCP), a paraphyletic group of unicellular algae at the base of chlorophytes, have been shown to associate with PSI-LHCI supercomplexes in *Ostreococcus tauri* (189), in which Lhcp1 and Lhcp2 form trimers (81) despite the lack of a canonical trimer motif (102). Each LHCP contains eight Chls *a*, five Chls *b*, one Chl c_2–like pigment, four dihydroluteins, two prasinoxanthins, and one neoxanthin (81). As suggested previously (8, 189), LHCPs may also associate with PSII through the trimer formation. In another prasinophyte, *Pycnococcus provasolii*, LHCP transcript expression is strongly upregulated under orange- and blue-light illumination recognized by the Dualchrome1 photoreceptor (122). LHCPs are also found in *Mesostigma viride*, an early diverging streptophyte alga, suggesting that LHCPs have been lost during the evolution from streptophyte algae to embryophytes (8).

2.4.6. Rhodophyte LHC protein and red lineage Chl *a/b*-binding-like protein. Rhodophytes are one of the most primitive photosynthetic eukaryotes, containing both cyanobacterial phycobilisomes as their PSII antenna system and LHC-type proteins denoted as LHCRs for PSI (209). Each LHCR contains 11–13 Chls *a* and 5 zeaxanthins (148). Another LHC protein restricted to the rhodophyte lineage, including diatoms, is identified as red lineage Chl *a/b*–binding-like protein (RedCAP) (58), which was recently found to associate with PSI, similar to LHCRs (219).

2.4.7. Fucoxanthin-chlorophyll protein. Diatoms are stramenopiles responsible for up to 40% of oceanic photosynthesis. They use FCPs, which are Chl *a/c*–binding LHC proteins with a high amount of fucoxanthin (13). A large number of FCP genes in diatoms have been described: *Lhcf*, *Lhcq*, *Lhcr*, *Lhcx*, *Lhcy*, and *Lhcz* (50, 106, 139). For *Thalassiosira pseudonana*, *Phaeodactylum tricornutum*, and *Chaetoceros gracilis*, there are 32, 35, and 46 FCP genes identified, respectively

(7, 18, 106). Among FCPs, Lhcx has been shown to play photoprotective roles in diatoms (9) and eustigmatophytes (145). The specific locations and functions for Lhcq, Lhcy, and Lhcz proteins so far are unknown. Lhcq has been previously described in chlorophytes (102) but is now identified as Lhcb7. A typical FCP contains 6 to 7 Chls *a*, 3 Chls *c*, and 6 fucoxanthins (203). Several FCP oligomeric conformations have been described in different diatom species—dimers (203, 224), trimers (13, 224), tetramers (131, 149), and nonamers (158).

2.4.8. Violaxanthin-chlorophyll protein. Although most stramenopiles contain Chl *a*/*c*–binding LHC proteins, eustigmatophytes lack Chl *c* in their LHC proteins, called violaxanthin-Chl proteins (VCPs). These VCPs (also known as Lhcvs) generally form a trimer (117) and contain Chl *a*, violaxanthin, and vaucheriaxanthin(-ester) for light-harvesting pigments with Car-Chl energy transfer efficiency over 90% (93). These Cars are located in the L1 and L2 sites and considered to play an important role in quenching triplet excited chlorophylls (^{3}Chls*) (26, 93).

2.5. LHC Proteins for Energy-Dependent Quenching

LHC proteins enable efficient energy transfer to photosystems without wasteful dissipation (167). However, excess energy can generate reactive oxygen species, causing photooxidative damage in photosynthetic proteins and membranes and lowering overall photosynthetic efficiency. Photosynthetic organisms have developed feedback mechanisms to switch between photosynthetic light harvesting and nonphotochemical quenching (NPQ), which functions in photoprotection to dissipate excess energy safely. Energy-dependent quenching (qE) is the fastest feedback mechanism among several known types of NPQ and is induced within seconds to minutes in response to HL. Mechanistic hypotheses have been proposed and described elsewhere (12, 161). We will describe how LHCs play essential roles in qE.

2.5.1. Pigment clusters involved in quenching excess energy. Light absorption by Chl generates the singlet excited state (^{1}Chl*), followed by ultrafast energy transfer to nearby Chls in LHCs. Absorption of excess light in HL increases the yield of intersystem crossing from ^{1}Chl* to the triplet excited state (^{3}Chl*), which can transfer energy to the triplet ground state of molecular oxygen to generate singlet oxygen ($^1O_2$*). While Cars can directly quench ^{3}Chl* and $^1O_2$* (2, 25), the Chl-Chl and Chl-Car clusters within LHC proteins can also keep the lifetime of ^{1}Chl* short by quenching excess energy in the first place. Pigment clusters, such as *a*603-lutein at L2, *b*606-*b*607, and *a*611-*a*612-lutein at L1 (**Figure 1*b–j***), are suggested to be sites of quenching within LHCII proteins, and conformational changes upon lumenal acidification could be the switch that activates quenching (45, 115, 160). Lumenal acidification also activates violaxanthin de-epoxidase, resulting in the replacement of violaxanthin by zeaxanthin in LHCs (136, 138). In addition to zeaxanthin's antioxidant capacity (70), Chl-zeaxanthin clusters can form a charge-transfer state to quench excess energy (77, 144).

2.5.2. Aggregation-induced quenching in LHCII. To study LHCII proteins in vitro, detergents are used to solubilize and stabilize these membrane proteins. Remarkable fluorescence quenching was observed in LHCII upon removal of detergents in vitro, which causes LHCII aggregation (163). In vitro LHCII aggregation is modulated by the charge of available lipids (165), local pH (147), and LHCII density (134), suggesting physiological factors such as zeaxanthin, lumen acidification, and protein environment may be potentiators of aggregation-induced quenching. However, evidence of LHCII aggregation in vivo has been restricted to freeze-fracture electron microscopy (EM) data (88) and artificial conditions such as in lincomycin-treated leaves depleted of their RCs (175). Better understanding of how LHCII aggregation may be regulated

Reactive oxygen species: damaging, reactive derivatives of oxygen (H_2O_2, O_2^-, $^1O_2$*) formed as byproducts during photosynthesis

Singlet excited state: a long-lived (~nanosecond order) excited state of Chl that results from the absorption of a photon or transfer of excitation energy from another pigment

in the thylakoid membrane and its response to HL will be essential in resolving the magnitude of its contribution to NPQ.

2.5.3. Energy-dissipative LHC proteins. Among the diverse LHC family, some have evolved to function in qE rather than light harvesting. Stress-related LHC proteins (LHCSRs) have three TM domains and are essential for qE in *Chlamydomonas* (146). LHCSR3 functions as both the site of qE and the sensor of HL through protonation at negatively charged residues upon lumenal acidification in HL (10, 16, 116, 146). The lack of LHCSR3 severely affects qE capacity, which is also dependent on the availability of lutein foremost, the LHC protein Lhcbm1 (57, 119), and zeaxanthin (16, 137, 195). Based on biochemical reconstitution studies, LHCSR3 can bind 7–8 Chls (with a much higher affinity for Chl *a* than Chl *b*) and 2–3 Cars (one lutein and one violaxanthin/zeaxanthin) (10, 16). LHCSR3 can interact with both PSI and PSII, depending on the redox state of the plastoquinone pool and function in quenching at both sites (6). While LHCSRs do not exist in tracheophytes (102), the bryophyte *Physcomitrium patens* (previously named as *Physcomitrella*) contains a zeaxanthin-dependent LHCSR1 (4, 152). Similar to *Chlamydomonas* LHCSR3, *Physcomitrium* LHCSR1 can associate with both PSI and PSII and function in qE (151).

LHCSR family proteins known as Lhcxs are found in haptophytes and stramenopiles, but not in rhodophytes or cryptophytes, and are essential for qE in diatoms (9, 21, 190) and eustigmatophytes (145). Although the qE capacity of Lhcx proteins in diatoms strongly depends on the availability of diatoxanthin (13, 21), how they interact seems unclear (63) but may be coordinated through a tryptophan located in the second TM domain (20). In contrast to LHCSRs, Lhcx proteins do not appear to sense the lumenal acidification through conserved protonatable residues (20, 63).

The qE capacity in the eustigmatophyte *Nannochloropsis oceanica*, lacking Chl *c* and lutein, also strongly depends on LHCX1 and the availability of zeaxanthin rather than diatoxanthin (145). Ultrafast spectroscopy has resolved two distinct qE mechanisms involving Chl *a* and zeaxanthin: (*a*) excitation energy transfer quenching through de-excitation of a Chl-zeaxanthin cluster and (*b*) charge-transfer quenching through the formation of a Chl-zeaxanthin radical cation followed by charge recombination.

2.5.4. Photosystem II subunit S. Previously identified as a 22-kDa subunit (or CP22), PSII subunit S (PsbS) is another member of the LHC superfamily found in Viridiplantae. Unlike other LHCs, PsbS contains four TM domains (TM1–TM4), in which TM1 and TM3 are oriented in the same way as in helices A and B of LHCII. TM2 (equivalent to helix C in LHCII) is located near one side of the central core TM1/TM3 structure, and TM4 is located on the other side of the core structure, making the structure compact without internal space for accommodating pigments (59). In vitro reconstitution experiments show that PsbS does not bind pigment (17), though molecular dynamics simulations suggest possible intermolecular coordination of Cars between PsbS and LHCs (44). PsbS contributes additively to qE in bryophytes along with LHCSR (4) and is essential for qE in embryophytes (110). The abundance of the PsbS polypeptide is also correlated with qE capacity (112). Moreover, mutation of two protonation sites on the lumenal domains causes the complete lack of qE capacity, suggesting that PsbS functions as the sensor of HL (111). PsbS is hypothesized to form a dimer in low light (59), where protonation induces conformational changes of these lumenal domains that may cause monomerization (103, 114). In contrast to embryophytes, the PsbS in *Chlamydomonas* accumulates only transiently after HL exposure and appears to play an indirect role in qE (5, 33), possibly through reorganizing thylakoid structures and LHCs (157). Despite a significant amount of research, the exact role of PsbS in qE and its location around PSII are still unclear.

3. ANTENNA PLASTICITY OF PHOTOSYSTEM I

PSI is a multisubunit pigment-binding protein complex responsible for catalytic light-induced oxidation of plastocyanin and reduction of ferredoxin leading to the production of NADPH. The core structures of PSI are highly conserved from cyanobacteria to tracheophytes, with flexible and surprisingly diverse PSI antenna systems. In cyanobacteria, PSI can form varied oligomeric conformations to increase functional antenna size—monomers (34), dimers (29), trimers (69, 91), and tetramers—driven in part by structural variation in the PsaL subunit (109, 225). A member of the CBP family (see the sidebar titled Different Types of Light-Harvesting Antenna Systems), called iron stress-induced A (IsiA) protein, which is homologous to the PSII subunit CP43, can function as cyanobacterial antennae by forming supercomplexes with variable numbers of IsiAs: 6 of them can associate with the PSI monomer (129), and 18 of them can localize around a PSI trimer as a ring (24, 198). The largest known supercomplex consists of 43 IsiA monomers forming a double-ring structure around a PSI trimer (216). Functional antenna size adjustment without LHCs in cyanobacteria reflects strategies to maximize the functional capacity of limited, iron-rich PSI under nutrient stress—an early innovation in regulating excitation energy flow that preceded the expansion of LHCI.

3.1. Diverse Antenna Organization of Eukaryotic Photosystem I

LHCI proteins form dimers, and the dimers can associate laterally with each other, forming an LHCI belt (tetramer). Each chlorophyte PSI contains up to 10 LHCIs (**Figure 2*a*,*b***), creating a double-layered belt made of 8 LHCIs (belt 1/belt 2) on the PsaA/PsaB/PsaF/PsaJ side and an LHCI dimer associating with the PsaB/PsaI side (153, 185). The bryophyte *Physcomitrium* forms a modified PSI-LHCI structure through the binding of Lhcb9 to PsaK, whose LHCI belt 2 is rotated ∼73° counterclockwise toward the PsaK side (**Figure 2*c***). An LHCII trimer binds to PsaO/PsaK, Lhcb9, and the edge of belt 2 (82, 150, 186, 221). By contrast, embryophytes only have 4 LHCIs associated with the PsaB/PsaF/PsaJ/PsaA side, forming a single-layered belt (154) (**Figure 2*d***). The association of an LHCII trimer with PSI is mediated through the phosphorylated N-terminal domain, which occurs in chlorophytes and tracheophytes during state transitions (78, 142, 143).

In a primitive rhodophyte, *Cyanidioschyzon merolae*, 3 LHCRs are associated with the PsaA/PsaJ/PsaK side of PSI, and an LHCR dimer associates with the other PsaL/PsaI/PsaM side (148) (**Figure 2*i***). In another rhodophyte, *Porphyridium purpureum*, 7 LHCRs and 1 RedCAP surround PSI with an opening on the PsaL/PsaO/PsaK side (219) (**Figure 2*j***). In cryptophytes, an ancient group derived from rhodophytes via secondary endosymbiosis, up to 14 alloxanthin-Chl *a*/*c*–binding proteins (ACPIs) surround PSI, in which another unique one-helix ACP, called ACPI-S, stabilizes a double-layer ACPI assembly (223) (**Figure 2*k***). The biggest eukaryotic PSI antenna organization observed so far is in the diatom *Chaetoceros* with 24 FCPs (212) (**Figure 2*l***). The structurally consistent yet positionally variable LHCI belt structure may highlight an efficient strategy for regulating PSI light harvesting, with a degree of flexibility that accommodates variation in light and thylakoid membrane environments.

3.2. Photosystem I Subunits for Binding of LHC Proteins in the Green Lineage

There are nine evolutionarily conserved eukaryotic PSI subunits—PsaA–PsaF, PsaI, PsaJ, and PsaL. PsaM is found in cyanobacteria, rhodophytes (148, 219), chlorophytes (28, 81, 153), and bryophytes (65, 186, 221), but not in tracheophytes. PsaG, PsaH, PsaO, and PsaN first appear within chlorophytes (81), but the absence of PsaH (and CrLhca2) allows some PSI dimerization in

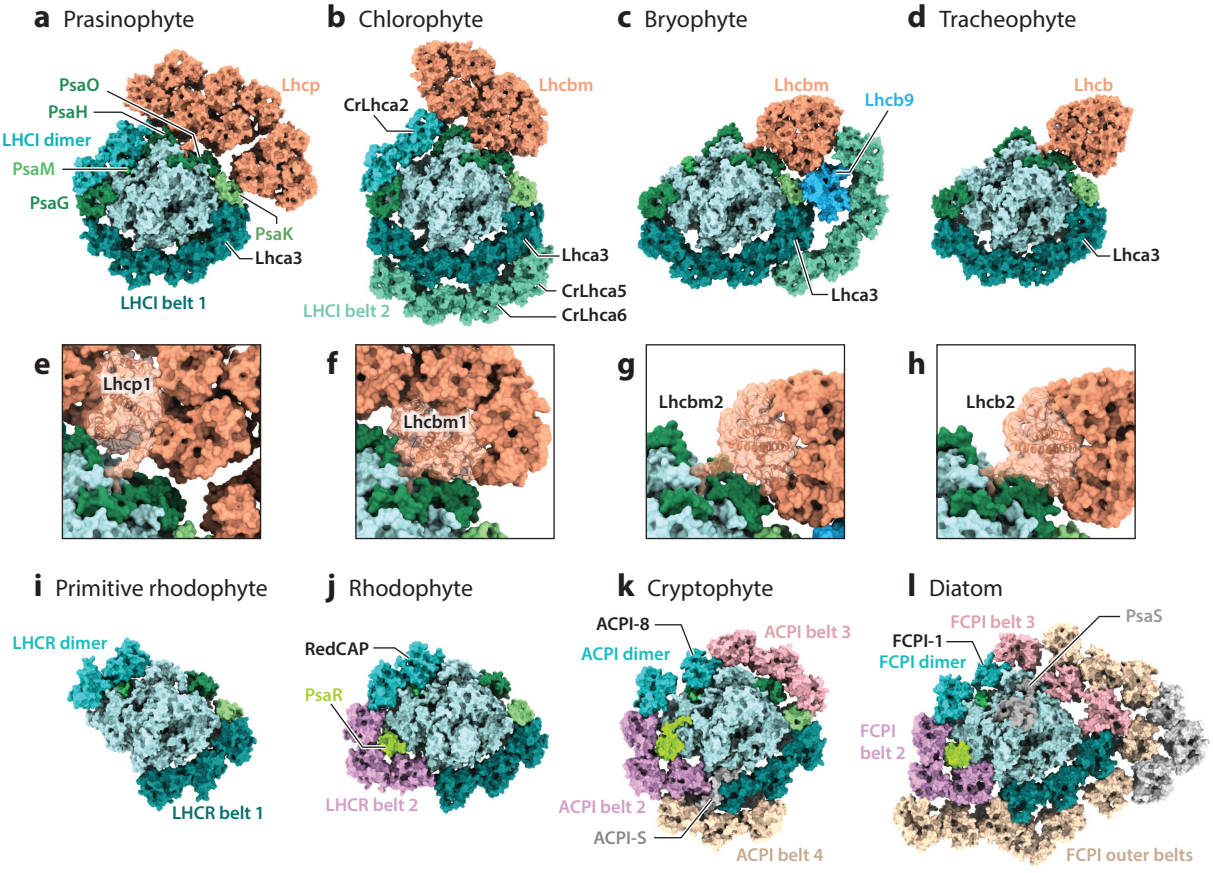

Figure 2

Diverse antenna organization of PSI supercomplexes in different species. (*a*) The prasinophyte *Ostreococcus tauri* (PDB ID 7YCA), (*b*) the chlorophyte *Chlamydomonas reinhardtii* (PDB ID 7D0J), (*c*) the bryophyte *Physcomitrium patens* (PDB ID 7XQP), (*d*) the tracheophyte *Zea mays* (PDB ID 5ZJI), and (*e–h*) the close-up views of each of their phosphorylated LHCII trimers, respectively. (*i*) The primitive rhodophyte *Cyanidioschyzon merolae* (PDB ID 5ZGB), (*j*) the rhodophyte *Porphyridium purpureum* (PDB ID 7Y5E), (*k*) the cryptophyte *Chroomonas placoidea* (PDB ID 7Y7B), and (*l*) the diatom *Chaetoceros gracilis* (PDB ID 6LY5). Only protein density is shown. Key antenna proteins and PSI subunits are labeled. The other subunits and repetitive labels are omitted for the clarity of the figures. Abbreviations: ACPI, alloxanthin-chlorophyll protein of PSI; FCPI, fucoxanthin-chlorophyll protein of PSI; LHC, light-harvesting complex; LHCI, LHC proteins of PSI; LHCII, LHC proteins of PSII; PDB ID, Protein Data Bank identifier; PSI, photosystem I; PSII, photosystem II; RedCAP, red lineage chlorophyll *a/b*–binding-like protein. Figure created using UCSF ChimeraX (124).

Chlamydomonas (132). Rhodophytes also acquired PsaO and PsaR. Diatoms acquired PsaS but lost PsaK and PsaO after secondary endosymbiosis. PsaX is absent in all photosynthetic eukaryotes.

3.2.1. The first layer, LHCI belt 1. In streptophytes, PsaG is associated with PsaB at the opposite location to PsaK associated with PsaA. PsaG serves as an anchor for LHCI association. Based on *Arabidopsis* mutant studies, the stable association between these PSI subunits and LHCIs is highly dependent on structural affinity, as PsaG and PsaK associate only with AtLhca1 and AtLhca3, respectively (206). AtLhca1 forms a stable heterodimer with AtLhca4, and AtLhca3 with AtLhca2, forming an LHCI belt 1 near PsaG/PsaF/PsaJ/PsaK, where each heterodimer mediates energy transfer to PSI (207). AtLhca1 and AtLhca3 can form another heterodimer

with the lowly abundant LHCIs AtLhca5 and AtLhca6 substituting for AtLhca4 and AtLhca2, respectively, which assemble the LHCI belt that specifically mediates the protein–protein interaction with the chloroplast NADH-dehydrogenase-like complex (171, 182). Although the lack of PsaG or PsaK affects the stability of LHCI association, there are only marginal effects on photosynthetic growth even without both PsaG and PsaK (201). The lack of each LHCI does not show a significant growth defect either, except for the lack of AtLhca4, which destabilizes AtLhca1/AtLhca2/AtLhca3 (95). The insignificant impact on growth even without these PSI subunits and LHCIs might reflect PSI resiliency and robustness, possibly through complementary antenna adjustment by recruiting LHCIIs (32).

Both AtLhca1–AtLhca4 and AtLhca2–AtLhca3 heterodimers contain Chls *a* with lower energy states than typical Chls, emitting fluorescence at ∼730 nm at low temperature (205). AtLhca3 and AtLhca4 contain Chls with the lowest energy states, which are generated by the charge-transfer states formed via the specific interaction between two Chls (*a*603/*a*609) maintained by the asparagine near *a*603 (36). *Physcomitrium* lacks the ortholog of AtLhca4, but its PSI still has the LHCI belt, in which a paralog, PpLhca2, substitutes for AtLhca4 (65, 186, 221). Because PpLhca2 does not contain low energy-state Chls, the lack of an AtLhca4 ortholog in *Physcomitrium* PSI causes its fluorescence emission to be ∼10 nm shorter than that observed in tracheophyte PSI (65). In *Chlamydomonas*, CrLhca2, CrLhca4, and CrLhca9 also show similar interactions with Chl *a*603, exhibiting the lowest energy states maintained by the nearby asparagine, although its fluorescence emission is ∼10 nm shorter than that observed in tracheophyte PSI (127). In *Ostreococcus*, OtLhca5 and OtLhca6 have a similar *a*603-*a*609 dimeric interaction with the asparagine as in CrLhca2/CrLhca9. However, its PSI lacks a fluorescence emission peak at longer wavelengths, likely due to a different pigment environment resulting from the tyrosine residues near *a*609 in OtLhca5/OtLhca6, instead of tryptophan residues in CrLhca2/CrLhca9 (81).

Lhca3 appears to be the only LHCI protein unique to Viridiplantae and has a specific role in binding to the PsaA/PsaK side of PSI (27, 28, 78, 81, 142, 154, 185) (**Figure 2*a–d***). The N-terminal domain of Lhca3 is distinct from other LHCIs, which enables a close interaction with PsaK. The longer flexible region (5–10 additional residues) before helix B makes a tight interaction with PsaA. In *Chlamydomonas*, the RNA interference knockdown of CrLhca3 caused a severe reduction of most LHCIs, except for CrLhca2 and CrLhca9 (which are located on the PsaB/PsaH/PsaI side) (133). Intriguingly, N-terminal processing of CrLhca3 has been observed under iron-deficient conditions (133), generating a shorter CrLhca3 that is not resolved in *Chlamydomonas* PSI structures. The corresponding N-terminal region for *C. ohadii* Lhca3 is resolved and shows a hydrophilic helix (28), which has similar helical propensities to that of CrLhca3. It is thus possible that N-terminal processing under iron-deficient conditions removes this hydrophilic helix and causes antenna reorganization (133). In fact, another chlorophyte, *Dunaliella salina*, induces thylakoid iron deficiency-induced protein (TIDI), which associates with PSI under iron-deficient conditions (202). Based on sequence analysis, TIDI has a high similarity to Lhca3 but a higher molecular weight of ∼30 kDa (46). The exact location of the TIDI-binding site and the mechanism for how it functions in remodeling PSI antenna organization under iron-deficient conditions remain to be determined.

3.2.2. An additional LHCI dimer. PSI can possess another LHCI dimer on the PsaB/PsaH/PsaI side, which is observed mainly in chlorophyte PSI (81, 183, 185) (**Figure 2*a*,*b***). What promotes the binding of another LHCI dimer to this location seems to be unclear. In some chlorophytes (e.g., *Bryopsis corticulans*, *C. ohadii*, and *Ostreococcus*), another PSI subunit, PsaM, which is located at the periphery of PsaB and next to PsaI, contributes to the protein–protein interaction with the LHCI dimer (e.g., BcLhca-i/BcLhca-j, CoLhca2/CoLhca9, or OtLhca5/OtLhca6) (28, 81, 153). On the other hand, PSI from at least two other chlorophytes, *Chlamydomonas* and

Dunaliella, lost the PsaM subunit, but the LHCI dimer (CrLhca2/CrLhca9, DsLhca5/DsLhca6) still binds to the same location (27, 183, 185), although chain X is observed in the PsaM site in *Chlamydomonas* (183). Intriguingly, one LHCI within the dimer on the side of PsaL (i.e., BcLhca-j, CoLhca2, OtLhca6, CrLhca2, and DsLhca5) is found to have a fourth TM domain, called helix F, thus exposing both the N- and C-terminal ends to the stroma. Helix F is positioned parallel to helix C of the adjacent LHCI (i.e., BcLhca-i, CoLhca9, OtLhca5, CrLhca9, and DsLhca6), showing tight hydrophobic interactions between each other. Whether helix F promotes the interaction with PsaM needs to be determined experimentally, as the four-helix LHCI is found regardless of the presence of PsaM.

Neither a four-helix LHCI nor PsaM has been found in tracheophytes, but *Arabidopsis* PSI can also harbor an Lhca1–Lhca4 heterodimer at the same side, although it is located closer to the PsaI/PsaH/PsaL site held with a LHCII trimer associated at the PsaH/PsaL/PsaO site (35). Although PsaM is found in the bryophyte *Physcomitrium* PSI, the binding of an additional LHCI heterodimer at the PsaB/PsaI/PsaH/PsaL side has not been observed even with the binding of an LHCII trimer at the PsaH/PsaL/PsaO site (186, 221), which might be due to the lack of an Lhca4 ortholog in *Physcomitrium*. Due to its structural plasticity, the exact function of this additional, yet conserved, LHCI dimer remains unknown.

3.2.3. The docking site for LHCII proteins. On the periphery of PsaA, another PSI subunit, PsaO, exists between PsaL and PsaK (27, 28, 78, 81, 142, 143, 186, 221). The periphery of the PsaH/PsaL/PsaO side is known as the docking site for LHCII trimers in state transitions (86, 121). One LHCII trimer is associated with *Zea mays* PSI and *Physcomitrium* PSI, two LHCII trimers with *Chlamydomonas* PSI, and three LHCP trimers with *Ostreococcus* PSI (**Figure 2*a–d***). The binding to these LHC trimers is facilitated through the trimer's phosphorylated N-terminal domain (e.g., ZmLhcb2, PpLhcbm2, CrLhcbm1, and OtLhcp1). The interaction of the phosphorylated domain from each trimer extending into the hydrophobic cavity created by PsaH/PsaL/PsaO is remarkably conserved in each organism (**Figure 2*e–h***). Interestingly, how each trimer is oriented with PSI subunits is different, which may reflect the flexibility of this binding of the phosphorylated LHCII to this site. Based on two cryo-EM structures of *Chlamydomonas* PSI-LHCI-LHCII supercomplexes, the rotational shift of the trimer (CrLHCII-1) varies from ∼6° to ∼40° compared to the corresponding trimer in the *Zea* PSI-LHCI-LHCII supercomplex. The distance from the nearest Chl in PsaO to the nearest Chl (*a*611) in CrLHCII-1 ranges from ∼17 to ∼20 Å between the two PSI structures, which may indicate that such a degree of variation is insignificant for energy transfer from the LHCII to PSI.

In *Chlamydomonas* PSI (**Figure 2*b***), the second LHCII trimer (CrLHCII-2) can associate with PsaH and Lhca2 (78, 143). This binding is stabilized by three separate protein–protein interactions: (*a*) the phosphorylated N-terminal domain of CrLhcbm5 interacting with the three charged residues in PsaH (Lys60/Glu58/Asp64) that are not conserved in tracheophyte PsaH, (*b*) the AC loops and BC loops between Lhcbm5 and Lhca2 facilitated by MGDG on the lumenal side, and (*c*) the close interaction with CrLHCII-1. Phosphorylation of CrLhcbm5 has been shown in state transitions (state 2) (191), and the lack of CrLhcbm5 disrupts the binding of two trimers to PSI, suggesting its essential role in stabilizing the interaction of these two LHCIIs with PSI in *Chlamydomonas* (143).

In *Ostreococcus* PSI-LHCI-LHCP supercomplexes (**Figure 2*a***), phosphorylation of the N-terminal domain of OtLhcp1 mediates the interaction of three LHCP trimers on the periphery of PsaH/PsaL/PsaO/PsaK and OtLhca6 (81). Because of the unique trimeric LHCP structure, the trimer with the phosphorylated Lhcp1 (Trimer 2) localizes more toward the PsaH and OtLhca6 side. However, the phosphorylated N-terminal domain of Lhcp1 extends into the same

hydrophobic cavity created by PsaH/PsaL/PsaO, showing both high flexibility and high specificity of the phosphorylated N-terminal domain (**Figure 2*e***). This N-terminal domain appears to contact closely with the next trimer (Trimer 1), which does not have direct contact with PsaO. The third trimer (Trimer 3) is associated with PsaK and is also in close contact with Trimer 1 through the extended lumenal BC loops of each structure.

3.2.4. The second layer, LHCI belt 2. Some chlorophytes have PSI-LHCI supercomplexes that form a double-layered LHCI structure composed of eight LHCIs (belt 1 and belt 2). So far, PSIs from *Chlamydomonas*, *Bryopsis*, and *C. ohadii* have been shown to form double LHCI belts (28, 78, 143, 153, 185). Based on *Chlamydomonas* LHCI nomenclature (185), the inner belt 1 consists of CrLhca1a/CrLhca8/CrLhca7/CrLhca3, and the outer belt 2 consists of CrLhca1b/CrLhca4/CrLhca6/CrLhca5, listed from the PsaG to the PsaK side. What stabilizes the double-belt formation appears to be the CrLhca6/CrLhca5 heterodimer (**Figure 2*b***), which interacts strongly with the CrLhca7/CrLhca3 heterodimer through unusually long C-terminal domains of CrLhca6/CrLhca5, forming a long hairpin loop on the lumenal side that binds additional Chls and Cars in the gap between the inner and outer LHCI belts. The lack of CrLhca5 destabilizes the formation of the double belt (140). Based on a Basic Local Alignment Search Tool (BLAST) search, such a uniquely long C-terminal domain does not exist in any LHCI proteins in tracheophytes and may underlie the absence of belt 2 in tracheophytes.

The uniquely oriented LHCI belt 2 in *Physcomitrium* PSI is stabilized by Lhcb9, a *Physcomitrium*-specific LHC protein (3), and a phosphorylated LHCII trimer associated with PsaH/PsaL/PsaO via the phospho-threonine in the N-terminal domain of PpLhcbm2 in the same way as in *Zea* PSI (186, 221). Lhcb9 appears to hold the entire antenna complex together as it interacts with PsaK, the LHCII trimer, and the inner and outer LHCI belts. The lack of Lhcb9 causes dissociation of LHCI belt 2 and the LHCII trimer due to its multiple interactions with surrounding subunits (84, 150).

3.3. Antenna Expansion of Photosystem I in the Red Lineage

Although much less is known about PSI antenna systems in the red lineage as compared to the ones in the green lineage, recent advancements in cryo-EM studies have provided structural insight into how LHCRs have expanded the antenna systems around PSI in the red lineage.

3.3.1. Rhodophyte photosystem I antenna systems. In addition to nine evolutionarily conserved eukaryotic PSI subunits (PsaA–PsaF, PsaI, PsaJ, and PsaL), the primitive rhodophyte *Cyanidioschyzon* PSI contains PsaO, PsaM, and PsaK but lacks PsaG and PsaH. Whereas four LHCIs exist in LHCI belt 1 in Viridiplantae PSI, three LHCRs bind to the PsaJ/PsaA/PsaK side in *Cyanidioschyzon* (148) (**Figure 2*i***). Also, *Cyanidioschyzon* PSI contains an LHCR dimer (CmLhcr1*/CmLhcr2*) at the PsaB/PsaM/PsaI/PsaL side. Compared to *Chlamydomonas* PSI, the binding location of the LHCR dimer is more toward PsaL because of the lack of PsaH (148, 185). In another rhodophyte, *Porphyridium purpureum*, PsaR is located in the same site as PsaG in Viridiplantae PSI, which assembles three more LHCRs around it (219) (**Figure 2*j***). *Porphyridium* PSI also contains an LHCR dimer composed of PpLhcr2 and PpRedCAP; the former associates with PsaM, and the latter forms a tighter interaction with PsaM/PsaI/PsaL than CmLhcr1* does. Therefore, five and eight LHCRs are associated in *Cyanidioschyzon* PSI and *Porphyridium* PSI, respectively, but the PsaL/PsaO/PsaK side for both is empty (**Figure 2*i,j***). An unknown linker protein was found near the PsaA/PsaO site in *Porphyridium* PSI, which binds tightly with the PSII subunit PsbO on the lumenal side, mediating interaction between PSI and PSII that appears to stabilize the formation of PSI-PSII megacomplexes (219). Interestingly, a similar PSI-PSII megacomplex formation has also been observed in *Arabidopsis* without a linker protein (217).

3.3.2. Cryptophyte photosystem I antenna systems. PsaR is also found in the cryptophyte *Chroomonas placoidea* PSI, and it is likely derived from rhodophytes via secondary endosymbiosis (223). *Chroomonas* PSI has up to 14 ACPIs, 8 of which are positioned at locations similar to those of the 8 LHCRs in *Porphyridium* PSI (**Figure 2*k***). ACPI-8 has a distinct characteristic from other ACPIs and resembles the RedCAP found in *Porphyridium* PSI (e.g., the protein sequence, the amphipathic helix at the N-terminal region on the stromal side, the Chl-binding sites, and the protein positioned at the PsaM/PsaI/PsaL). Thus, it is most likely that ACPI-8 is an ortholog of RedCAP. Although they appear to bind very loosely, 3 ACPIs localize at the periphery of the PsaL/PsaO/PsaK side of the *Chroomonas* PSI (belt 3). Out of 14 total ACPIs, 11 surround *Chroomonas* PSI. Interestingly, the remaining 3 ACPIs form the outer layer belt (belt 4) with the help of ACPI-S, a previously uncharacterized protein, which mediates the association between the inner and outer layers of ACPIs. *Chroomonas* ACPIs preferentially form trimers rather than dimers, as there are 4 sets of 3 ACPIs associated laterally with a highly similar antenna organization (223).

3.3.3. Diatom photosystem I antenna systems. Compared to rhodophyte PSI, diatom PSI has acquired PsaS but lacks PsaK/PsaO (7, 18). *Chaetoceros* PSI can have up to 24 FCPIs, forming an inner layer with 11 FCPIs, a middle layer with 10 FCPIs, and an outer layer with 3 FCPIs (130, 212) (**Figure 2*l***). The inner FCPI belts are similar in structure to the *Chroomonas* ACPI belts, except for 3 FCPIs (belt 3) on the periphery of the PsaL/PsaA side due to the lack of PsaO/PsaK in *Chaetoceros* PSI. Although the N-terminal structure of FCPI-1, which is found in the same location as the RedCAP in *Porphyridium* PSI (219) and *Chroomonas* ACPI-8 (223), is not well resolved, the overall orientation of 3 TM helices, the C-terminal amphipathic helix, Chl-binding sites, and the predicted sequence have high similarity to each other (212), suggesting that *Chaetoceros* FCPI-1 is likely a RedCAP ortholog. Most of the inner FCPI belts have high structural similarity with rhodophyte LHCRs, while most in the outer belts are Lhcf or Lhcq proteins (106, 212). Two FCPIs in the outer belts (FCPI-14/FCPI-16) have a long N-terminal domain and BC loop, both of which interact with the FCPIs in the outer layer. The FCPIs most distant from PSI (FCPI-21/FCPI-23/FCPI-24) also have a unique hydrophilic helix at the N-terminal region and 3 long loop structures at the AC loop, BC loop, and C-terminal regions, indicating that these flexible domains have important roles in protein–protein interactions. Interestingly, the red lineage RedCAP/ACPI-8/FCPI-1 and the chlorophyte 4-helix LHCI (e.g., CrLhca2) both mediate PSI interactions with the PsaB/PsaI-side LHCI/LHCR/ACPI/FCPI dimer. The effect of this structure on LHCI light harvesting and the reason behind its evolutionary loss in land plants are still unclear.

4. ANTENNA HIERARCHIES OF PHOTOSYSTEM II

PSII is the multisubunit pigment-binding protein complex responsible for catalytic light-induced water oxidation and plastoquinone reduction. The 4 large PSII subunits, D1 (PsbA), D2 (PsbD), CP43 (PsbC), and CP47 (PsbB), assemble the main body with multiple small transmembrane subunits (12–15, depending on species) and the lumenal oxygen-evolving complex as the membrane-extrinsic subunits. PSII is mainly found as a dimer, whereas PSII monomers and associated auxiliary proteins are involved in PSII assembly or repair (43), with strong conservation across photosynthetic organisms. For example, the PSII subunits PsbI and PsbM, which seem to have arisen during the evolution of cyanobacteria (155), are important for the formation of PSII dimers (92). The rapid and efficient turnover of photodamaged PSII relative to PSI may have evolved to protect PSI that is slowly assembled de novo (196). In contrast to PSI, PSII is a potent photosensitizer that must balance robust light harvesting and photoprotection.

CP43 and CP47 are the most proximal light-harvesting antenna proteins for the PSII RC. PSII can form supercomplexes composed of various numbers of LHCIIs (23, 54). In most

tracheophytes, three monomeric LHCIIs, CP24 (*LHCB6*), CP26 (*LHCB5*), and CP29 (*LHCB4*), are located adjacent to the PSII RC. The most abundant LHCII proteins, generally called major LHCIIs, form trimers composed of Lhcb1, Lhcb2, and/or Lhcb3 (85). In chlorophytes and bryophytes, their major LHCIIs are designated as Lhcbm (m meaning major) and have relatively low protein sequence similarity to Lhcbs in tracheophytes (3, 57, 83). PSII-LHCII supercomplexes can also associate with each other, forming megacomplexes (100). To accommodate rearrangements during light harvesting, photoprotection, and PSII repair, LHCII must be exceptionally dynamic in both its protein–protein interactions and capacity for translocation within and across the thylakoid membrane.

4.1. What Governs Photosystem II–LHCII Associations?

Because cyanobacteria do not possess LHCs for PSII, the structural features that enabled the evolution of PSII–LHCII associations in photosynthetic eukaryotes are of great interest. The most stable PSII supercomplex observed in Viridiplantae is the so-called C_2S_2 supercomplex, in which two CP26 proteins, two CP29 proteins, and two strongly bound LHCII trimers, or S-LHCIIs (S_2), associate with a PSII core dimer (C_2). PSII has three contact sites for LHCII binding: CP43–CP26, CP47–CP29, and PsbW–S-LHCII. CP26 and CP29 are thought to bind more tightly to PSII than does S-LHCII based on differences during PSII core complex purification (125).

4.1.1. CP43–CP26 contact site. CP26 binds to CP43 similarly across chlorophytes and tracheophytes (170, 173, 184, 204) (**Figure 3*a*,*b***). On the stromal side, the N-terminal domain of CP26 has a close interaction with CP43 and PsbZ, which also plays an essential role in binding CP26. On the lumenal side, the C-terminal amphipathic helix of CP26 binds with PsbZ. Several Chls, one Car, and lipids fill in the interface between CP43, PsbZ, and CP26, forming a strong connection through hydrophobic interactions. The lack of PsbZ causes a severe reduction of the CP26 protein level, which also impedes PSII-LHCII supercomplex formation and photoprotection (188). Variation in the contact site between the N-terminal domains of CP26 and an S-LHCII monomer likely contributes to modest differences in the CP43–S-LHCII junction between chlorophytes and tracheophytes (172).

4.1.2. CP47–CP29 contact site. The N-terminal domain of CP29 has a unique extended loop structure, which binds to the stromal surface of CP47 through hydrogen bonds and van der Waals interactions (170, 173, 184, 204) (**Figure 3*a*,*b***). The N-terminal domain of PsbH is associated with the stromal end of helix B of CP29, and the subsequent N-terminal loop connected to the TM domain of PsbH is interposed between the main bodies of CP29 and CP47 (**Figure 4*a*,*b***). A similar protein–protein interaction is observed in diatom PSII structures, which lack CP29; instead, the N-terminal domain of PsbG forms a loop structure and associates on the stromal surface of CP47, connecting an FCP tetramer to PSII (131, 149) (**Figures 3*c*** and **4*c*,*d***). Curiously, PSII assembly intermediate complexes from *Thermosynechococcus* spp. show the binding of an assembly factor, Psb34 (or Tsl0063), which exhibits a protein–protein interaction via an extended loop structure on the stromal surface of CP47 (210, 220) (**Figure 4*e*,*f***), similar to how CP29 interacts with CP47. Moreover, a linker protein (named $L_{PP}1$) connecting the phycobilisome and PSII has a similar interaction between its C-terminal end and the stromal surface of CP47, as observed in *Porphyridium* (219) (**Figure 4*g*,*h***). These different examples of an interaction between peripheral proteins and CP47/PsbH suggest that the stromal surface of CP47 might serve as a binding platform for proteins with an elongated loop structure that has been co-opted during evolution for functions as diverse as PSII assembly and light harvesting.

4.1.3. PsbW–S-LHCII contact site. PsbW is located at the periphery of CP43 together with PsbI, which is closely associated with D1 (**Figure 3*a*,*b***). The interaction between PsbW and

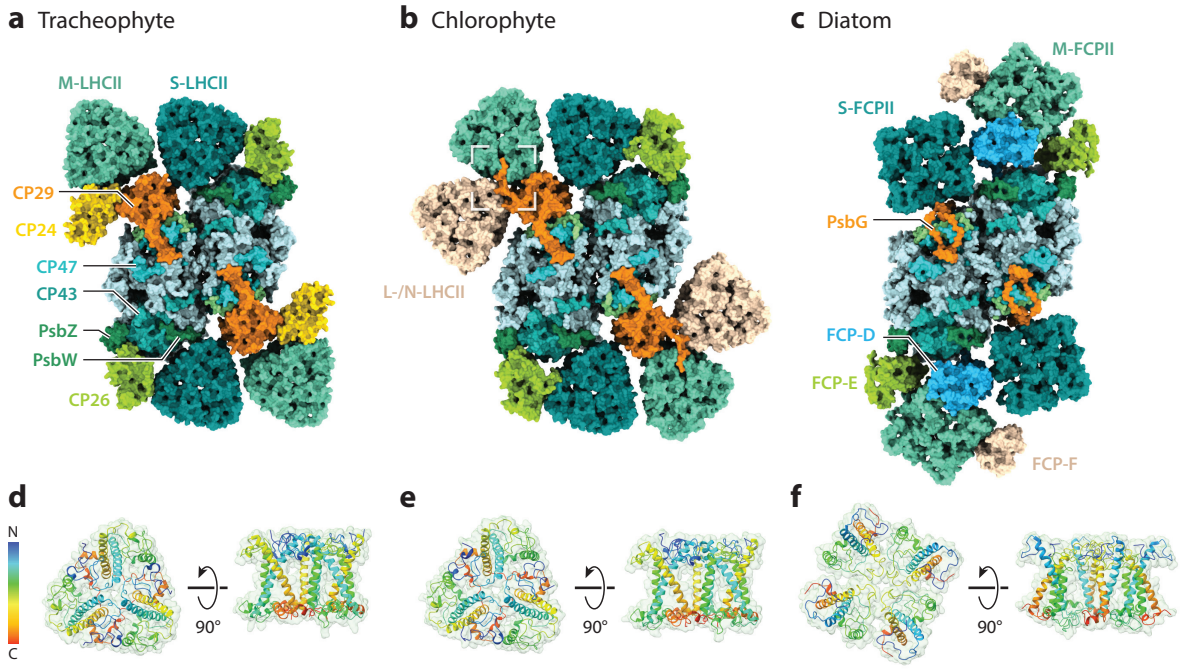

Figure 3

Antenna organization in PSII supercomplexes from (*a*) the tracheophyte *Pisum sativum* (PDB ID 5XNL), (*b*) the chlorophyte *Chlamydomonas reinhardtii* (PDB ID 6KAD), and (*c*) the diatom *Chaetoceros gracilis* (PDB ID 6JLU). Only protein density is shown. The unique N-terminal domain of chlorophyte CP29, which has close contact with M- and L-/N-LHCIIs, is indicated by the box in panel *b*. Note that each model is refined with C2 symmetry. Key antenna proteins and PSII subunits are labeled. (*d–f*) The top and side views of S-LHCII from panels *a* and *b* and S-FCPII from panel *c* are shown with ribbon diagrams color-coded from the N- to C-terminal ends. The labels for the other subunits and repetitive labels are omitted for the clarity of the figures. Abbreviations: FCPII, fucoxanthin-chlorophyll proteins of PSII; LHCII, light-harvesting complex proteins of photosystem II; PDB ID, Protein Data Bank identifier; PSII, photosystem II. Figure created using UCSF ChimeraX (124).

S-LHCII is mediated by thylakoid lipids (either PG or DGDG) located between them (170, 173, 184, 204). One of the lipids is in close contact with CP43, which stabilizes the binding of S-LHCII at that position. On the lumenal side, helix D of a monomer within S-LHCII has a close interaction with an amphipathic helix of CP43. In addition, there are two tight interactions between another monomer within S-LHCII and CP26 through their stromal (AC loop regions) and lumenal (BC loop regions) domains. It is of note that CP26 is not essential for the binding of S-LHCII at that location (214), whereas the lack of PsbW destabilizes the formation of PSII supercomplexes and causes a disordered PSII organization in thylakoid membranes (62). However, PsbW may have only a small functional effect on PSII activity because (*a*) cyanobacterial PSII lacks PsbW, (*b*) rhodophyte PSII contains PsbW even though LHCII is absent (1), and (*c*) the lack of PsbW causes no significant growth phenotype in embryophytes, suggesting compensatory mechanisms that sustain photosynthetic efficiency (62).

4.2. Additional LHCII Trimers That Increase Photosystem II Antenna Size

At least one more LHCII trimer can associate stably with a PSII supercomplex. A moderately bound LHCII trimer, or M-LHCII, forms the so-called $C_2S_2M_1$ supercomplex, in which M-LHCII binds next to S-LHCII and CP29 on one side (170, 173, 184) (**Figure 3*a*,*b***). To improve structural resolution, most published PSII-LHCII supercomplexes are refined with

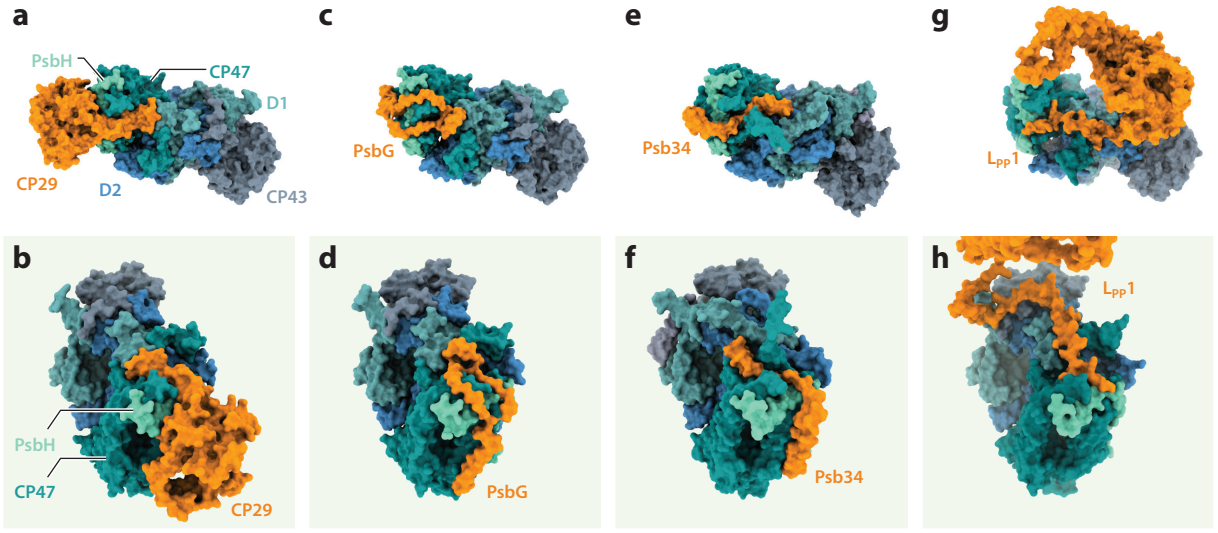

Figure 4

Different instances of protein–protein interactions involving CP47. (*a*,*b*) The protein–protein interaction between CP47/PsbH and CP29 observed in Viridiplantae PSII supercomplexes. The *Pisum* PSII structure (PDB ID 5XNL) is shown. (*c*,*d*) The protein–protein interaction between CP47/PsbH and PsbG, which is unique to the diatom PSII supercomplexes and connects with an FCP tetramer. The *Chaetoceros* PSII structure (PDB ID 6JLU) is shown. (*e*,*f*) The protein–protein interaction between CP47/PsbH and Psb34 (or Tsl0063), which is a PSII assembly factor observed in cyanobacteria PSII assembly intermediate complexes. The *Thermosynechococcus* PSII assembly intermediate (PDB ID 7NHP) is shown. (*g*,*h*) The protein–protein interaction between CP47/CP43/D1/D2 and $L_{PP}1$, a linker protein connecting the phycobilisome and PSII observed in rhodophytes. The *Porphyridium* PSII structure (PDB ID 7Y5E) is shown. Panels *a*, *c*, *e*, and *g* show stromal-side views. Panels *b*, *d*, *f*, and *h* show side-angled views. Only D1, D2, CP43, CP47, and PsbH are shown for PSII core complexes for the clarity of the figures. The repetitive labels are omitted for the clarity of the figures. Abbreviations: FCP, fucoxanthin-chlorophyll protein; PDB ID, Protein Data Bank identifier; PSII, photosystem II. Figure created using UCSF ChimeraX (124).

C2 symmetry (based on the assumption that the structure has a twofold symmetry). Thus, the $C_2S_2M_2$ supercomplex is commonly known as the next level of PSII supercomplexes, even though it is less frequently observed than the $C_2S_2M_1$ supercomplex in most cases. Whether such asymmetric PSII antenna organizations are meaningful or caused by spontaneous loss during sample preparation needs to be determined.

4.2.1. CP29–CP24–M-LHCII. According to the PhycoCosm database as of June 2023 (**https://phycocosm.jgi.doe.gov/phycocosm/home**), CP24 is found in some streptophyte algae (e.g., *Klebsormidium*) and tracheophytes (except for Pinaceae and Gnetales) (99) but not in chlorophytes or rhodophytes. CP24 has a longer AC loop on the stromal side, which interacts strongly with the N-terminal domain of CP29 (184). There is also a close contact site between the lumenal side of helix C of CP24 and the C-terminal domain of CP29. Three Cars are bound at the L1, L2, and N1 sites of CP24, and the one at the N1 site stabilizes the interaction with CP29, which resembles the interaction observed in LHCI heterodimers. The CP29–CP24 dimer appears to serve as the binding site for M-LHCII, which is a heterotrimer containing Lhcb1, Lhcb2, and Lhcb3 (23). Exceptionally, CP26 can form heterotrimers with Lhcb3 when Lhcb1 and Lhcb2 are absent (162). The Lhcb3 in M-LHCII is responsible for binding CP24 through both stromal (between helix A of Lhcb3 and the elongated AC loop of CP24) and lumenal domains (between the BC loops of each).

Like CP24, Lhcb3 also arose in the streptophyte lineage after their divergence from chlorophytes. Therefore, it is tempting to assume that both LHCs are important for the binding of

M-LHCII. However, the gymnosperm *Picea* (Pinaceae) and *Gnetum* (Gnetales) genomes have lost both CP24 and Lhcb3 but still retain M-LHCII in the *Picea* PSII-LHCII supercomplex, which rotates ~52° to increase the area of association with S-LHCII (99). Because of such rotation of M-LHCII and the lack of CP24, the overall shape of the $C_2S_2M_2$ supercomplex is quite different from those of other tracheophytes and is thus called the spruce-type PSII supercomplex. The spruce-type $C_2S_2M_1$ supercomplex can be formed in *Arabidopsis* PSII supercomplexes lacking Lhcb3 and/or CP24, albeit at low abundance and with weak binding of the M-LHCII (80).

Interestingly, the lack of CP29 destabilizes CP24 (47). The lack of CP24, on the other hand, slightly increases the amount of CP29 (48, 101). The lack of Lhcb3 does not significantly change the abundance of CP24 or CP29 in the thylakoid membrane (42). The *Arabidopsis* mutant lines lacking CP29, CP24, or Lhcb3 still show the formation of C_2S_2 supercomplexes (23, 42, 47, 80, 101). The lack of stable binding of M-LHCII to PSII does not seem to affect photosynthetic growth, but the lack of CP24 causes a slower growth rate than that of the wild type due to a slower rate of electron transfer caused by altered PSII macro-organization in thylakoid membranes (48, 101).

4.2.2. Chlorophyte CP29 and the binding of additional LHCII trimers. CP24 is not found in chlorophytes, but a larger PSII supercomplex has been observed in *Chlamydomonas*, which is further evidence that CP24 is not an absolute requirement for the binding of additional LHCII trimers to PSII. In addition to M-LHCII, *Chlamydomonas* PSII contains an L-/N-LHCII (loosely bound or naked LHCII) (170, 173) (**Figure 3*b***). An interesting difference in the binding of M-LHCII is observed in the N-terminal domain of CP29, which extends toward M-LHCII and also has a close interaction with the L-/N-LHCII on the stromal side (173). M-LHCII rotates about 50–60° to increase the area of association with S-LHCII. On the lumenal side, helix D of CP29 has a close contact with the BC loop of a monomer within both M-LHCII and L-/N-LHCII. Thus, CP29 is responsible for the binding of both M-LHCII and L-/N-LHCII without CP24 in chlorophytes. A similar association of the M- and L-/N-LHCIIs with PSII is also observed in the spruce-type PSII supercomplexes without CP24 (99, 100). According to the draft genome (v1.0) of *Picea abies* (187), its CP29 (MA_129206g0010) has high similarity to *Arabidopsis* CP29 and does not possess the linker motif (RSGGVGYRKY) found in the N-terminal end of *Chlamydomonas* CP29, which connects to the M- and L-/N-LHCIIs. It will be interesting to determine how the binding of these LHCIIs in the spruce-type PSII supercomplexes is stabilized without CP24 or the linker motif of CP29.

4.3. Antenna Evolution of Photosystem II in the Red Lineage

It is still not clear what controls the preferential association of different LHC proteins with PSI or PSII. Cryo-EM structures of PSII supercomplexes in the red lineage are becoming more available, providing important insights into how unique protein structures of their PSII subunits and LHCs give rise to specific protein–protein interactions. During the revision of this manuscript, new cryo-EM structures from a centric diatom, *Cyclotella meneghiniana*, were published (224), which we do not cover in detail due to space constraints. In brief, the structures show monomeric, dimeric, and trimeric FCP proteins of PSII (FCPIIs), in addition to tetrameric FCPIIs as described in Section 4.3.2, indicating the diverse nature of FCPIIs and their unique associations with PSII.

4.3.1. Rhodophyte photosystem II antenna systems. Although rhodophyte PSI uses LHC-type proteins (LHCRs), rhodophytes are considered to be relatively primitive photosynthetic eukaryotes because their PSII uses a cyanobacteria-derived phycobilisome as a light-harvesting antenna (see the sidebar titled Different Types of Light-Harvesting Antenna Systems). While several PSII subunits [PsbA (D1), PsbB (CP47), PsbC (CP43), PsbD (D2), PsbE (α-subunit of

cytochrome b_{559}), PsbF (β-subunit of cytochrome b_{559}), PsbH, PsbI, PsbJ, PsbK, and PsbL] are conserved from cyanobacteria to tracheophytes, some distinctive differences exist in rhodophyte PSII (e.g., the oxygen-evolving complex and some small subunits) (1). Interestingly, rhodophyte PSII dimers can associate with each other, forming an oligomeric conformation with up to a pentamer of dimers (219). On the stromal side of PSII, five linker proteins connect to the phycobilisome. One of these linkers ($L_{PP}1$) also stabilizes the interaction between PSII and PSI, forming a PSII-PSI megacomplex.

4.3.2. Diatom photosystem II antenna systems. PSII from the diatom *Chaetoceros gracilis* has a very similar subunit composition to the one in rhodophytes, with the addition of newly identified subunit PsbG (149). This diatom PSII can form supercomplexes with two sets of three FCPII monomers (named FCP-D, FCP-E, and FCP-F) and two sets of two FCPII tetramers (131, 149) (**Figure 3*c***). The strongly bound FCPII tetramer, S-FCPII, binds on the CP47 side via PsbG, whose sequence is not yet available as of June 2023 but contains an N-terminal domain loop structure attached on the stromal surface of CP47 that somewhat resembles the CP29–CP47 interaction in Viridiplantae. On the CP43 side, two FCPII monomers (FCP-D and FCP-E) directly associate with PSII and connect the moderately bound FCPII tetramer, or M-FCPII, on the outer side. FCP-D is the largest FCP in the supercomplex because of its long loops in both its N-terminal and C-terminal domains. The long N-terminal domain of FCP-D directly associates with both CP43 and M-FCPII on the stromal side, while the C-terminal domain forms an extended loop structure on the lumenal side of CP43 and has close contact with PsbW on the lumenal side. FCP-D was recently identified as Lhcr17 and is the only FCPII protein belonging to the LHCR subfamily (106). FCP-E also connects to M-FCPII with CP43 through the AC loop, which is in close contact with PsbZ, and helix C, which has hydrophobic interactions with M-FCPII. The last monomer, FCP-F, is located farthest outside the supercomplex and is associated closely with M-FCPII. It is of interest that the diatom PSII uses the same subunits for interacting with antenna proteins as the Viridiplantae PSII: PsbZ for FCP-E (or CP26), PsbW for FCP-D (or S-LHCII), and CP47 for PsbG (or CP29). Overall, the binding of S-/M-FCPIIs to PSII is indirectly stabilized by those three subunits, and Chls and Cars appear to be essential for the interactions between them.

Compared to Viridiplantae LHCIIs, diatom FCPIIs appear to have several differences that may underlie their tetrameric versus trimeric structure: (*a*) the N-terminal domain of FCPII is much shorter (at least within the resolved region) than that of LHCII; (*b*) the orientation of helices A and B of FCPII is opposite (i.e., the stromal side of helices A and B faces outward and inward for LHCII, respectively, but the stromal side of helices A and B faces inward and outward for FCPII, respectively) (**Figure 3*d–f***); (*c*) the longer AC loop of FCPII allows more flexible interaction at the center part of the tetramer on the stromal side; and (*d*) the C-terminal domain of FCPII is shorter and faces outward, creating a larger space between each FCPII (which is filled with Cars). Though orthologous in their LHCII-stabilizing function, significant structural differences between FCP-E and CP26, FCP-D and S-LHCII, and PsbG and CP29 likely also contribute to the tetramer and trimer structures in the red and green lineages, respectively. Because the pigment compositions between LHCII and FCPII are largely different (131, 149), such tetrameric interactions might also be preferable for energy transfer and quenching mechanisms specific to FCPII (203).

4.4. Photosystem II Antenna Dynamics and Its Photoprotective Role in Angiosperms

The binding of these LHCIIs to PSII, including the dynamic reorganization of multimeric LHCII in response to HL (94), is considered to not only increase the efficiency of light absorption but

also regulate photoprotection. For detailed discussion about photoprotective mechanisms, please see other recent reviews (e.g., 12, 161).

The lack of each LHCII monomer has distinct effects on NPQ in *Arabidopsis*. The lack of CP26 does not cause significant differences in either the induction or magnitude of NPQ but results in slightly faster NPQ relaxation than in the wild type (48). The lack of CP29 (which also causes the loss of CP24) reduces the overall magnitude of NPQ with a slower gradual increase of NPQ than in the wild type (47). The lack of CP24 results in unique NPQ kinetics: a quick induction with stable maintenance of NPQ lacking any gradual increase in HL (48). Curiously, the double knockout of CP24 and CP26 regains its capacity for NPQ induction over time (48). This result is explained by the level of PSII ordered arrays. The C_2S_2 supercomplexes lacking CP24 form tightly packed arrays, whereas the double knockout of CP24 and CP26 regains spaces between the supercomplexes (48). The lack of CP29 (and CP24) also reduces the formation of PSII crystalline arrays (47, 64). Thus, crowded PSII environments with fewer areas for LHCII to move around appear to hinder the gradual induction of NPQ. Intriguingly, the lack of PsbS generates more frequent PSII crystalline arrays than the wild type, but the overexpression of PsbS causes the lack of crystalline array formation, suggesting that PsbS also affects the interactions between PSII supercomplexes (64).

A correlation between NPQ induction levels and the formation of an LHCII subcomplex composed of CP29–CP24–M-LHCII (named B4C) has been observed in *Arabidopsis* (15). When the NPQ level is high, B4C disappears, suggesting that the subcomplex is dissociated into monomers and M-LHCII. The dissociation of B4C is not observed in the absence of PsbS or its protonation even under HL. Thus, PsbS protonation is correlated with the dissociation of B4C, most likely via a direct interaction between them. Moreover, HL induces dissociation of LHCII from PSII and aggregation of LHCII (15, 88). An intriguing empty site near CP24/CP29 observed in the $C_2S_2M_2$ supercomplex has been suggested as a possible PsbS-binding site upon its monomerization under HL (59, 184). In summary, the PsbS-dependent B4C dissociation is considered to cause dynamic rearrangement of PSII antenna systems for photoprotection.

An extensive amount of research has been done to pinpoint the site(s) of NPQ in land plants. The *Arabidopsis NoM* mutant lacking CP24, CP26, and CP29 shows a substantially slower NPQ induction than does the wild type but eventually reaches similar NPQ levels (40). However, a mutant lacking all major LHCIIs shows a ~60% reduction of NPQ with similar induction and relaxation kinetics as compared to the wild type (135). Among all deletion mutants observed, the lack of PsbS (*npq4*) or the lack of zeaxanthin and lutein (*npq1 lut2*) causes the most significant abolishment of NPQ capacity (110, 111). It has been shown that high levels of ΔpH induced by artificial mediators of cyclic electron transfer (i.e., diaminodurene) can induce wild-type levels of NPQ in isolated chloroplasts of PsbS mutants, suggesting that PsbS is essential for LHCII quenching under physiologically relevant conditions, but it can be bypassed at unnaturally low lumen pH values (89). However, it is still unclear how protonation of PsbS could affect the apparent pK_a of qE occurring in LHCII. Further research on structural and functional features underlying PsbS–LHCII interactions and quenching may help resolve the detailed role of PsbS in modulating qE.

5. OPPORTUNITIES FOR TRANSLATION OF RESEARCH ON LHC PROTEINS

Over hundreds of millions of years, photosynthetic eukaryotes have evolved versatile LHCs that augment the conserved cores of PSI and PSII. Their success cannot be overstated—from the assorted functions of OHPs to LHCs, the diversification of various LHC-type proteins across species, and the proliferation of LHC copy numbers within species, these organisms have evolved

myriad strategies to optimize photosynthesis, plasticity, and robustness in diverse environments. Widespread tolerance of redundant LHCs has fostered opportunities for neofunctionalization. It is also clear that there is no one-size-fits-all solution, as showcased by desert extremophiles such as *C. obadii* that substitute ∼50% of Chl *b* for Chl *a* in LHCIs to maintain fitness in extreme HL (28) and clades such as the gymnosperms that have evolved structural alternatives for PSII supercomplexes in the absence of highly conserved land plant CP24 and Lhcb3 orthologs (99).

LHC proteins drive photosynthetic adaptation. Thus, they are prime targets for genetic engineering. Multiple promising studies already exist, such as in the heterologous biosynthesis of Chl *c* in planta (87), the functional in vitro integration of Chl *d* in land plant LHCII (56), and efforts to accelerate the kinetics of NPQ to enhance photosynthetic efficiency and yield in field-grown crops (49, 105). Comparative structural studies can underpin successes like these, resolving flexible and essential protein features and assessing the fitness potential of different LHC strategies. Better understanding of the pigment networks that underlie efficient excitation energy transfer and photoprotection will help resolve structure-function trade-offs. Genetic manipulation based on LHC structural data shows significant promise to enhance light-harvesting efficiency in diverse organisms, from biofuel algae to crop plants.

SUMMARY POINTS

1. The evolution of light-harvesting complex (LHC) proteins has facilitated the expansion of photosynthetic eukaryotes into almost all ecological niches.
2. The characteristic α-helical core of LHC proteins has maintained functional conservation in structure and pigment-binding capacity, with flexible loop regions mediating key protein–protein interactions.
3. The LHC superfamily functions beyond light harvesting, supporting a wide array of functions that improve photosynthetic efficiency (e.g., formation of supercomplexes, altered absorption spectra, and photoprotection).
4. LHC-based antenna structures first arose at photosystem I (PSI), and they show significant extant variation in supercomplex size, shape, and oligomer density across photosynthetic eukaryotes despite retention of characteristic structures such as the LHCI belts and dimers.
5. The photosensitivity of photosystem II (PSII) has necessitated the expansion of photoprotection and dissipative energy pathways in LHCII.
6. Strong conservation of photosystem reaction centers has been leveraged in a variety of ways, such as in the recurring use of CP47 as a docking site for diverse protein–protein interactions in LHCII.
7. The robustness and adaptability of LHC proteins make them a prime candidate for bioengineering efforts to redesign photosynthesis.

FUTURE ISSUES

1. The trade-offs of single-particle averaging: Ångström-resolution cryo-electron microscopy structures require the statistical power behind single-particle averaging of hundreds of thousands of particles. However, low-abundance and dynamic structures

are potentially averaged out. While software and hardware advances have been made to increase the resolution of key protein–protein interactions and protein dynamics, it is important that the raw and processed output of these computational tools is interpreted carefully and thoroughly. Specific sample preparation will often be necessary to reveal unique protein–protein interactions and correlate structural observations with mechanistic understanding.

2. Molecules beyond protein structures: The structural determination of pigments and lipids, and their orientation within and between protein complexes, is crucial in understanding energy transfer pathways and photoprotection mechanisms. Little is known about dynamic interactions between pigments and LHC proteins that could occur transiently in response to stress conditions such as high light. A combination of spectroscopy, pigment analysis, and biochemistry could help interpret structural data and overcome limitations in pigment and lipid identification in single-particle analysis.
3. Effective use of in silico models: With significant advances in predictive structural algorithms (e.g., AlphaFold) and molecular dynamics simulations, there is even greater capacity for computational modeling of dynamic protein interactions with pigments, lipids, and other proteins. However, these models are only as effective as the assumptions used in making them. Such analyses would benefit from critically evaluating multiple and contrasting hypotheses and avoiding biases. Validation of model results by genetic perturbation may remain the gold standard in translating new findings.

DISCLOSURE STATEMENT

The authors are not aware of any affiliations, memberships, funding, or financial holdings that might be perceived as affecting the objectivity of this review.

ACKNOWLEDGMENTS

We apologize to all the colleagues whose work we could not cite and/or discuss extensively in this review due to space constraints. This work was supported by the US Department of Energy Office of Science, through the Photosynthetic Systems program in the Office of Basic Energy Sciences. K.K.N. is an investigator of the Howard Hughes Medical Institute.

LITERATURE CITED

1. Ago H, Adachi H, Umena Y, Tashiro T, Kawakami K, et al. 2016. Novel features of eukaryotic photosystem II revealed by its crystal structure analysis from a red alga. *J. Biol. Chem.* 291(11):5676–87
2. Agostini A, Nicol L, Da Roit N, Bortolus M, Croce R, Carbonera D. 2021. Altering the exciton landscape by removal of specific chlorophylls in monomeric LHCII provides information on the sites of triplet formation and quenching by means of ODMR and EPR spectroscopies. *Biochim. Biophys. Acta Bioenerg.* 1862(11):148481
3. Alboresi A, Caffarri S, Nogue F, Bassi R, Morosinotto T. 2008. In *silico* and biochemical analysis of *Physcomitrella patens* photosynthetic antenna: identification of subunits which evolved upon land adaptation. *PLOS ONE* 3(4):e2033
4. Alboresi A, Gerotto C, Giacometti GM, Bassi R, Morosinotto T. 2010. *Physcomitrella patens* mutants affected on heat dissipation clarify the evolution of photoprotection mechanisms upon land colonization. *PNAS* 107(24):11128–33

5. Allorent G, Lefebvre-Legendre L, Chappuis R, Kuntz M, Truong TB, et al. 2016. UV-B photoreceptor-mediated protection of the photosynthetic machinery in *Chlamydomonas reinhardtii*. *PNAS* 113(51):14864–69
6. Allorent G, Tokutsu R, Roach T, Peers G, Cardol P, et al. 2013. A dual strategy to cope with high light in *Chlamydomonas reinhardtii*. *Plant Cell* 25(2):545–57
7. Armbrust EV, Berges JA, Bowler C, Green BR, Martinez D, et al. 2004. The genome of the diatom *Thalassiosira pseudonana*: ecology, evolution, and metabolism. *Science* 306(5693):79–86
8. Aso M, Matsumae R, Tanaka A, Tanaka R, Takabayashi A. 2021. Unique peripheral antennas in the photosystems of the streptophyte alga *Mesostigma viride*. *Plant Cell Physiol*. 62(3):436–46
9. Bailleul B, Rogato A, de Martino A, Coesel S, Cardol P, et al. 2010. An atypical member of the light-harvesting complex stress-related protein family modulates diatom responses to light. *PNAS* 107(42):18214–19
10. Ballottari M, Truong TB, De Re E, Erickson E, Stella GR, et al. 2016. Identification of pH-sensing sites in the light harvesting complex stress-related 3 protein essential for triggering non-photochemical quenching in *Chlamydomonas reinhardtii*. *J. Biol. Chem.* 291(14):7334–46
11. Bassi R, Croce R, Cugini D, Sandonà D. 1999. Mutational analysis of a higher plant antenna protein provides identification of chromophores bound into multiple sites. *PNAS* 96(18):10056–61
12. Bassi R, Dall'Osto L. 2021. Dissipation of light energy absorbed in excess: the molecular mechanisms. *Annu. Rev. Plant Biol.* 72:47–76
13. Beer A, Gundermann K, Beckmann J, Büchel C. 2006. Subunit composition and pigmentation of fucoxanthin–chlorophyll proteins in diatoms: evidence for a subunit involved in diadinoxanthin and diatoxanthin binding. *Biochemistry* 45(43):13046–53
14. Belgio E, Duffy CDP, Ruban AV. 2013. Switching light harvesting complex II into photoprotective state involves the lumen-facing apoprotein loop. *Phys. Chem. Chem. Phys.* 15(29):12253–61
15. Betterle N, Ballottari M, Zorzan S, de Bianchi S, Cazzaniga S, et al. 2009. Light-induced dissociation of an antenna hetero-oligomer is needed for non-photochemical quenching induction. *J. Biol. Chem.* 284(22):15255–66
16. Bonente G, Ballottari M, Truong TB, Morosinotto T, Ahn TK, et al. 2011. Analysis of LhcSR3, a protein essential for feedback de-excitation in the green alga *Chlamydomonas reinhardtii*. *PLOS Biol.* 9(1):e1000577
17. Bonente G, Howes BD, Caffarri S, Smulevich G, Bassi R. 2008. Interactions between the photosystem II subunit PsbS and xanthophylls studied in vivo and in vitro. *J. Biol. Chem.* 283(13):8434–45
18. Bowler C, Allen AE, Badger JH, Grimwood J, Jabbari K, et al. 2008. The *Phaeodactylum* genome reveals the evolutionary history of diatom genomes. *Nature* 456(7219):239–44
19. Büchel C. 2020. Light harvesting complexes in chlorophyll *c*-containing algae. *Biochim. Biophys. Acta Bioenerg.* 1861(4):148027
20. Buck JM, Kroth PG, Lepetit B. 2021. Identification of sequence motifs in Lhcx proteins that confer qE-based photoprotection in the diatom *Phaeodactylum tricornutum*. *Plant J.* 108(6):1721–34
21. Buck JM, Sherman J, Bártulos CR, Serif M, Halder M, et al. 2019. Lhcx proteins provide photoprotection via thermal dissipation of absorbed light in the diatom *Phaeodactylum tricornutum*. *Nat. Commun.* 10(1):4167
22. Caffarri S, Croce R, Breton J, Bassi R. 2001. The major antenna complex of photosystem II has a xanthophyll binding site not involved in light harvesting. *J. Biol. Chem.* 276(38):35924–33
23. Caffarri S, Kouřil R, Kereïche S, Boekema EJ, Croce R. 2009. Functional architecture of higher plant photosystem II supercomplexes. *EMBO J.* 28(19):3052–63
24. Cao P, Cao D, Si L, Su X, Tian L, et al. 2020. Structural basis for energy and electron transfer of the photosystem I–IsiA–flavodoxin supercomplex. *Nat. Plants* 6:167–76
25. Carbonera D, Agostini A, Bortolus M, Dall'Osto L, Bassi R. 2022. Violaxanthin and zeaxanthin may replace lutein at the L1 site of LHCII, conserving the interactions with surrounding chlorophylls and the capability of triplet–triplet energy transfer. *Int. J. Mol. Sci.* 23(9):4812
26. Carbonera D, Agostini A, Di Valentin M, Gerotto C, Basso S, et al. 2014. Photoprotective sites in the violaxanthin-chlorophyll *a* binding protein (VCP) from *Nannochloropsis gaditana*. *Biochim. Biophys. Acta Bioenerg.* 1837(8):1235–46

27. Caspy I, Malavath T, Klaiman D, Fadeeva M, Shkolnisky Y, Nelson N. 2020. Structure and energy transfer pathways of the *Dunaliella salina* photosystem I supercomplex. *Biochim. Biophys. Acta Bioenerg.* 1861(10):148253
28. Caspy I, Neumann E, Fadeeva M, Liveanu V, Savitsky A, et al. 2021. Cryo-EM photosystem I structure reveals adaptation mechanisms to extreme high light in *Chlorella ohadii*. *Nat. Plants* 7:1314–22
29. Chen M, Perez-Boerema A, Zhang L, Li Y, Yang M, et al. 2020. Distinct structural modulation of photosystem I and lipid environment stabilizes its tetrameric assembly. *Nat. Plants* 6:314–20
30. Chen M, Schliep M, Willows RD, Cai Z-L, Neilan BA, Scheer H. 2010. A red-shifted chlorophyll. *Science* 329(5997):1318–19
31. Chidgey JW, Linhartová M, Komenda J, Jackson PJ, Dickman MJ, et al. 2014. A cyanobacterial chlorophyll synthase-HliD complex associates with the Ycf39 protein and the YidC/Alb3 insertase. *Plant Cell* 26(3):1267–79
32. Chukhutsina VU, Liu X, Xu P, Croce R. 2020. Light-harvesting complex II is an antenna of photosystem I in dark-adapted plants. *Nat. Plants* 6:860–68
33. Correa-Galvis V, Redekop P, Guan K, Griess A, Truong TB, et al. 2016. Photosystem II subunit PsbS is involved in the induction of LHCSR protein-dependent energy dissipation in *Chlamydomonas reinhardtii*. *J. Biol. Chem.* 291(33):17478–87
34. Çoruh O, Frank A, Tanaka H, Kawamoto A, El-Mohsnawy E, et al. 2021. Cryo-EM structure of a functional monomeric photosystem I from *Thermosynechococcus elongatus* reveals red chlorophyll cluster. *Commun. Biol.* 4(1):304
35. Crepin A, Kučerová Z, Kosta A, Durand E, Caffarri S. 2020. Isolation and characterization of a large photosystem I–light-harvesting complex II supercomplex with an additional Lhca1–a4 dimer in Arabidopsis. *Plant J.* 102(2):398–409
36. Croce R, Chojnicka A, Morosinotto T, Ihalainen JA, van Mourik F, et al. 2007. The low-energy forms of photosystem I light-harvesting complexes: spectroscopic properties and pigment-pigment interaction characteristics. *Biophys. J.* 93(7):2418–28
37. Croce R, Muller MG, Bassi R, Holzwarth AR. 2001. Carotenoid-to-chlorophyll energy transfer in recombinant major light-harvesting complex (LHCII) of higher plants. I. Femtosecond transient absorption measurements. *Biophys. J.* 80(2):901–15
38. Crooks GE, Hon G, Chandonia J-M, Brenner SE. 2004. WebLogo: a sequence logo generator. *Genome Res.* 14:1188–90
39. Dall'Osto L, Bressan M, Bassi R. 2015. Biogenesis of light harvesting proteins. *Biochim. Biophys. Acta* 1847(9):861–71
40. Dall'Osto L, Cazzaniga S, Bressan M, Palecek D, Zidek K, et al. 2017. Two mechanisms for dissipation of excess light in monomeric and trimeric light-harvesting complexes. *Nat. Plants* 3:17033
41. Dall'Osto L, Cazzaniga S, North H, Marion-Poll A, Bassi R. 2007. The *Arabidopsis aba4-1* mutant reveals a specific function for neoxanthin in protection against photooxidative stress. *Plant Cell* 19(3):1048–64
42. Damkjær JT, Kereïche S, Johnson MP, Kovacs L, Kiss AZ, et al. 2009. The photosystem II light-harvesting protein Lhcb3 affects the macrostructure of photosystem II and the rate of state transitions in *Arabidopsis*. *Plant Cell* 21(10):3245–56
43. Danielsson R, Suorsa M, Paakkarinen V, Albertsson P-Å, Styring S, et al. 2006. Dimeric and monomeric organization of photosystem II: distribution of five distinct complexes in the different domains of the thylakoid membrane. *J. Biol. Chem.* 281(20):14241–49
44. Daskalakis V. 2018. Protein–protein interactions within photosystem II under photoprotection: the synergy between CP29 minor antenna, subunit S (PsbS) and zeaxanthin at all-atom resolution. *Phys. Chem. Chem. Phys.* 20(17):11843–55
45. Daskalakis V, Maity S, Hart CL, Stergiannakos T, Duffy CDP, Kleinekathöfer U. 2019. Structural basis for allosteric regulation in the major antenna trimer of photosystem II. *J. Phys. Chem. B* 123(45):9609–15
46. Davidi L, Gallaher SD, Ben-David E, Purvine SO, Fillmore TL, et al. 2023. Pumping iron: a multi-omics analysis of two extremophilic algae reveals iron economy management. *PNAS* 120(30):e2305495120
47. de Bianchi S, Betterle N, Kouril R, Cazzaniga S, Boekema E, et al. 2011. *Arabidopsis* mutants deleted in the light-harvesting protein Lhcb4 have a disrupted photosystem II macrostructure and are defective in photoprotection. *Plant Cell* 23(7):2659–79

48. de Bianchi S, Dall'Osto L, Tognon G, Morosinotto T, Bassi R. 2008. Minor antenna proteins CP24 and CP26 affect the interactions between photosystem II subunits and the electron transport rate in grana membranes of *Arabidopsis*. *Plant Cell* 20(4):1012–28
49. De Souza AP, Burgess SJ, Doran L, Hansen J, Manukyan L, et al. 2022. Soybean photosynthesis and crop yield are improved by accelerating recovery from photoprotection. *Science* 377(6608):851–54
50. Dittami SM, Michel G, Collén J, Boyen C, Tonon T. 2010. Chlorophyll-binding proteins revisited—a multigenic family of light-harvesting and stress proteins from a brown algal perspective. *BMC Evol. Biol.* 10(1):365
51. Dockter C, Müller AH, Dietz C, Volkov A, Polyhach Y, et al. 2012. Rigid core and flexible terminus: structure of solubilized light-harvesting chlorophyll *a/b* complex (LHCII) measured by EPR. *J. Biol. Chem.* 287(4):2915–25
52. Dolganov NA, Bhaya D, Grossman AR. 1995. Cyanobacterial protein with similarity to the chlorophyll *a/b* binding proteins of higher plants: evolution and regulation. *PNAS* 92(2):636–40
53. Domínguez-Martín MA, Sauer PV, Kirst H, Sutter M, Bína D, et al. 2022. Structures of a phycobilisome in light-harvesting and photoprotected states. *Nature* 609(7928):835–45
54. Drop B, Webber-Birungi M, Yadav SKN, Filipowicz-Szymanska A, Fusetti F, et al. 2014. Light-harvesting complex II (LHCII) and its supramolecular organization in *Chlamydomonas reinhardtii*. *Biochim. Biophys. Acta* 1837(1):63–72
55. Elias E, Liguori N, Croce R. 2023. At the origin of the selectivity of the chlorophyll-binding sites in Light Harvesting Complex II (LHCII). *Int. J. Biol. Macromol.* 243:125069
56. Elias E, Liguori N, Saga Y, Schäfers J, Croce R. 2021. Harvesting far-red light with plant antenna complexes incorporating chlorophyll *d*. *Biomacromolecules* 22(8):3313–22
57. Elrad D, Niyogi KK, Grossman AR. 2002. A major light-harvesting polypeptide of photosystem II functions in thermal dissipation. *Plant Cell* 14(8):1801–16
58. Engelken J, Brinkmann H, Adamska I. 2010. Taxonomic distribution and origins of the extended LHC (light-harvesting complex) antenna protein superfamily. *BMC Evol. Biol.* 10(1):233
59. Fan M, Li M, Liu Z, Cao P, Pan X, et al. 2015. Crystal structures of the PsbS protein essential for photoprotection in plants. *Nat. Struct. Mol. Biol.* 22(9):729–35
60. Fehr N, Dietz C, Polyhach Y, von Hagens T, Jeschke G, Paulsen H. 2015. Modeling of the N-terminal section and the lumenal loop of trimeric light harvesting complex II (LHCII) by using EPR. *J. Biol. Chem.* 290(43):26007–20
61. Formaggio E, Cinque G, Bassi R. 2001. Functional architecture of the major light-harvesting complex from higher plants. *J. Mol. Biol.* 314(5):1157–66
62. García-Cerdán JG, Kovács L, Tóth T, Kereïche S, Aseeva E, et al. 2011. The PsbW protein stabilizes the supramolecular organization of photosystem II in higher plants. *Plant J.* 65(3):368–81
63. Giovagnetti V, Jaubert M, Shukla MK, Ungerer P, Bouly J-P, et al. 2021. Biochemical and molecular properties of LHCX1, the essential regulator of dynamic photoprotection in diatoms. *Plant Physiol.* 188(1):509–25
64. Goral TK, Johnson MP, Duffy CD, Brain APR, Ruban AV, Mullineaux CW. 2012. Light-harvesting antenna composition controls the macrostructure and dynamics of thylakoid membranes in Arabidopsis. *Plant J.* 69(2):289–301
65. Gorski C, Riddle R, Toporik H, Da Z, Dobson Z, et al. 2022. The structure of the *Physcomitrium patens* photosystem I reveals a unique Lhca2 paralogue replacing Lhca4. *Nat. Plants* 8:307–16
66. Grimm B, Kloppstech K. 1987. The early light-inducible proteins of Barley. Characterization of two families of 2-h-specific nuclear-coded chloroplast proteins. *Eur. J. Biochem.* 167(3):493–99
67. Guo J, Zhang Z, Bi Y, Yang W, Xu Y, Zhang L. 2005. Decreased stability of photosystem I in *dgd1* mutant of *Arabidopsis thaliana*. *FEBS Lett.* 579(17):3619–24
68. Hagio M, Sakurai I, Sato S, Kato T, Tabata S, Wada H. 2002. Phosphatidylglycerol is essential for the development of thylakoid membranes in *Arabidopsis thaliana*. *Plant Cell Physiol.* 43(12):1456–64
69. Hamaguchi T, Kawakami K, Shinzawa-Itoh K, Inoue-Kashino N, Itoh S, et al. 2021. Structure of the far-red light utilizing photosystem I of *Acaryochloris marina*. *Nat. Commun.* 12(1):2333
70. Havaux M, Niyogi KK. 1999. The violaxanthin cycle protects plants from photooxidative damage by more than one mechanism. *PNAS* 96(15):8762–67

71. Hey D, Grimm B. 2018. ONE-HELIX PROTEIN2 (OHP2) is required for the stability of OHP1 and assembly factor HCF244 and is functionally linked to PSII biogenesis. *Plant Physiol*. 177(4):1453–72
72. Hey D, Grimm B. 2020. ONE-HELIX PROTEIN1 and 2 form heterodimers to bind chlorophyll in photosystem II biogenesis. *Plant Physiol*. 183(1):179–93
73. Hey D, Rothbart M, Herbst J, Wang P, Müller J, et al. 2017. LIL3, a light-harvesting complex protein, links terpenoid and tetrapyrrole biosynthesis in *Arabidopsis thaliana*. *Plant Physiol*. 174(2):1037–50
74. Hirashima M, Satoh S, Tanaka R, Tanaka A. 2006. Pigment shuffling in antenna systems achieved by expressing prokaryotic chlorophyllide *a* oxygenase in *Arabidopsis*. *J. Biol. Chem.* 281(22):15385–93
75. Hobe S, Förster R, Klingler J, Paulsen H. 1995. N-proximal sequence motif in light-harvesting chlorophyll *a/b*-binding protein is essential for the trimerization of light-harvesting chlorophyll *a/b* complex. *Biochemistry* 34(32):10224–28
76. Hofmann E, Wrench PM, Sharples FP, Hiller RG, Welte W, Diederichs K. 1996. Structural basis of light harvesting by carotenoids: peridinin-chlorophyll-protein from *Amphidinium carterae*. *Science* 272(5269):1788–91
77. Holt NE, Zigmantas D, Valkunas L, Li XP, Niyogi KK, Fleming GR. 2005. Carotenoid cation formation and the regulation of photosynthetic light harvesting. *Science* 307(5708):433–36
78. Huang Z, Shen L, Wang W, Mao Z, Yi X, et al. 2021. Structure of photosystem I-LHCI-LHCII from the green alga *Chlamydomonas reinhardtii* in State 2. *Nat. Commun.* 12(1):1100
79. Hutin C, Nussaume L, Moise N, Moya I, Kloppstech K, Havaux M. 2003. Early light-induced proteins protect *Arabidopsis* from photooxidative stress. *PNAS* 100(8):4921–26
80. Ilíková I, Ilík P, Opatíková M, Arshad R, Nosek L, et al. 2021. Towards spruce-type photosystem II: consequences of the loss of light-harvesting proteins LHCB3 and LHCB6 in Arabidopsis. *Plant Physiol*. 187(4):2691–715
81. Ishii A, Shan J, Sheng X, Kim E, Watanabe A, et al. 2023. The photosystem I supercomplex from a primordial green alga *Ostreococcus tauri* harbors three light-harvesting complex trimers. *eLife* 12:e84488
82. Iwai M, Grob P, Iavarone AT, Nogales E, Niyogi KK. 2018. A unique supramolecular organization of photosystem I in the moss *Physcomitrella patens*. *Nat. Plants* 4:904–9
83. Iwai M, Yokono M. 2017. Light-harvesting antenna complexes in the moss *Physcomitrella patens*: implications for the evolutionary transition from green algae to land plants. *Curr. Opin. Plant Biol.* 37:94–101
84. Iwai M, Yokono M, Kono M, Noguchi K, Akimoto S, Nakano A. 2015. Light-harvesting complex Lhcb9 confers a green alga-type photosystem I supercomplex to the moss *Physcomitrella patens*. *Nat. Plants* 1:14008
85. Jansson S. 1999. A guide to the *Lhc* genes and their relatives in *Arabidopsis*. *Trends Plant Sci*. 4(6):236–40
86. Jensen PE, Haldrup A, Zhang S, Scheller HV. 2004. The PSI-O subunit of plant photosystem I is involved in balancing the excitation pressure between the two photosystems. *J. Biol. Chem.* 279(23):24212–17
87. Jinkerson RE, Poveda-Huertes D, Cooney EC, Cho A, Ochoa-Fernandez R, et al. 2024. Biosynthesis of chlorophyll *c* in a dinoflagellate and heterologous production *in planta*. *Curr. Biol.* 34(3):594–605.e4
88. Johnson MP, Goral TK, Duffy CD, Brain AP, Mullineaux CW, Ruban AV. 2011. Photoprotective energy dissipation involves the reorganization of photosystem II light-harvesting complexes in the grana membranes of spinach chloroplasts. *Plant Cell* 23(4):1468–79
89. Johnson MP, Ruban AV. 2011. Restoration of rapidly reversible photoprotective energy dissipation in the absence of PsbS protein by enhanced ΔpH. *J. Biol. Chem.* 286(22):19973–81
90. Jumper J, Evans R, Pritzel A, Green T, Figurnov M, et al. 2021. Highly accurate protein structure prediction with AlphaFold. *Nature* 596(7873):583–89
91. Kato K, Shinoda T, Nagao R, Akimoto S, Suzuki T, et al. 2020. Structural basis for the adaptation and function of chlorophyll *f* in photosystem I. *Nat. Commun.* 11(1):238
92. Kawakami K, Umena Y, Iwai M, Kawabata Y, Ikeuchi M, et al. 2011. Roles of PsbI and PsbM in photosystem II dimer formation and stability studied by deletion mutagenesis and X-ray crystallography. *Biochim. Biophys. Acta Bioenerg.* 1807(3):319–25

93. Keşan G, Litvín R, Bína D, Durchan M, Šlouf V, Polívka T. 2016. Efficient light-harvesting using non-carbonyl carotenoids: energy transfer dynamics in the VCP complex from *Nannochloropsis oceanica*. *Biochim. Biophys. Acta Bioenerg.* 1857(4):370–79
94. Kim E, Watanabe A, Duffy CDP, Ruban AV, Minagawa J. 2020. Multimeric and monomeric photosystem II supercomplexes represent structural adaptations to low- and high-light conditions. *J. Biol. Chem.* 295(43):14537–45
95. Klimmek F, Ganeteg U, Ihalainen JA, van Roon H, Jensen PE, et al. 2005. Structure of the higher plant light harvesting complex I: in vivo characterization and structural interdependence of the Lhca proteins. *Biochemistry* 44(8):3065–73
96. Knoppová J, Sobotka R, Tichý M, Yu J, Konik P, et al. 2014. Discovery of a chlorophyll binding protein complex involved in the early steps of photosystem II assembly in *Synechocystis*. *Plant Cell* 26(3):1200–12
97. Konert MM, Wysocka A, Koník P, Sobotka R. 2022. High-light-inducible proteins HliA and HliB: pigment binding and protein–protein interactions. *Photosynth. Res.* 152(3):317–32
98. Kosugi M, Kawasaki M, Shibata Y, Hara K, Takaichi S, et al. 2023. Uphill energy transfer mechanism for photosynthesis in an Antarctic alga. *Nat. Commun.* 14(1):730
99. Kouřil R, Nosek L, Bartoš J, Boekema EJ, Ilík P. 2016. Evolutionary loss of light-harvesting proteins Lhcb6 and Lhcb3 in major land plant groups—break-up of current dogma. *New Phytol.* 210(3):808–14
100. Kouřil R, Nosek L, Opatíková M, Arshad R, Semchonok DA, et al. 2020. Unique organization of photosystem II supercomplexes and megacomplexes in Norway spruce. *Plant J.* 104(1):215–25
101. Kovács L, Damkjaer J, Kereïche S, Ilioaia C, Ruban AV, et al. 2006. Lack of the light-harvesting complex CP24 affects the structure and function of the grana membranes of higher plant chloroplasts. *Plant Cell* 18(11):3106–20
102. Koziol AG, Borza T, Ishida K-I, Keeling P, Lee RW, Durnford DG. 2007. Tracing the evolution of the light-harvesting antennae in chlorophyll *a/b*-containing organisms. *Plant Physiol.* 143(4):1802–16
103. Krishnan-Schmieden M, Konold PE, Kennis JTM, Pandit A. 2021. The molecular pH-response mechanism of the plant light-stress sensor PsbS. *Nat. Commun.* 12(1):2291
104. Król M, Spangfort MD, Huner NPA, Öquist G, Gustafsson P, Jansson S. 1995. Chlorophyll *a/b*-binding proteins, pigment conversions, and early light-induced proteins in a chlorophyll *b*-less barley mutant. *Plant Physiol.* 107(3):873–83
105. Kromdijk J, Głowacka K, Leonelli L, Gabilly ST, Iwai M, et al. 2016. Improving photosynthesis and crop productivity by accelerating recovery from photoprotection. *Science* 354(6314):857–61
106. Kumazawa M, Nishide H, Nagao R, Inoue-Kashino N, Shen J-R, et al. 2022. Molecular phylogeny of fucoxanthin-chlorophyll *a/c* proteins from *Chaetoceros gracilis* and Lhcq/Lhcf diversity. *Physiol. Plant.* 174(1):e13598
107. Kuttkat A, Hartmann A, Hobe S, Paulsen H. 1996. The C-terminal domain of light-harvesting chlorophyll-*a/b*-binding protein is involved in the stabilisation of trimeric light-harvesting complex. *Eur. J. Biochem.* 242(2):288–92
108. Levin G, Yasmin M, Liveanu V, Burstein C, Hanna R, et al. 2023. A desert *Chlorella* sp. that thrives at extreme high-light intensities using a unique photoinhibition protection mechanism. *Plant J.* 115:510–28
109. Li M, Calteau A, Semchonok DA, Witt TA, Nguyen JT, et al. 2019. Physiological and evolutionary implications of tetrameric photosystem I in cyanobacteria. *Nat. Plants* 5:1309–19
110. Li X-P, Björkman O, Shih C, Grossman AR, Rosenquist M, et al. 2000. A pigment-binding protein essential for regulation of photosynthetic light harvesting. *Nature* 403(6768):391–95
111. Li X-P, Gilmore AM, Caffarri S, Bassi R, Golan T, et al. 2004. Regulation of photosynthetic light harvesting involves intrathylakoid lumen pH sensing by the PsbS protein. *J. Biol. Chem.* 279(22):22866–74
112. Li X-P, Gilmore AM, Niyogi KK. 2002. Molecular and global time-resolved analysis of a *psbS* gene dosage effect on pH- and xanthophyll cycle-dependent nonphotochemical quenching in photosystem II. *J. Biol. Chem.* 277(37):33590–97
113. Li Y, Liu B, Zhang J, Kong F, Zhang L, et al. 2019. OHP1, OHP2, and HCF244 form a transient functional complex with the photosystem II reaction center. *Plant Physiol.* 179(1):195–208

114. Liguori N, Campos SRR, Baptista AM, Croce R. 2019. Molecular anatomy of plant photoprotective switches: the sensitivity of PsbS to the environment, residue by residue. *J. Phys. Chem. Lett.* 10(8):1737–42
115. Liguori N, Periole X, Marrink SJ, Croce R. 2015. From light-harvesting to photoprotection: structural basis of the dynamic switch of the major antenna complex of plants (LHCII). *Sci. Rep.* 5(1):15661
116. Liguori N, Roy LM, Opacic M, Durand G, Croce R. 2013. Regulation of light harvesting in the green alga *Chlamydomonas reinhardtii*: the C-terminus of LHCSR is the knob of a dimmer switch. *J. Am. Chem. Soc.* 135(49):18339–42
117. Litvín R, Bína D, Herbstová M, Gardian Z. 2016. Architecture of the light-harvesting apparatus of the eustigmatophyte alga *Nannochloropsis oceanica*. *Photosynth. Res.* 130(1):137–50
118. Liu L-N, Bracun L, Li M. 2024. Structural diversity and modularity of photosynthetic RC–LH1 complexes. *Trends Microbiol.* 32:38–52
119. Liu X, Nawrocki WJ, Croce R. 2023. The role of the pigment–protein complex LHCBM1 in nonphotochemical quenching in *Chlamydomonas reinhardtii*. *Plant Physiol.* 2023:kiad555
120. Liu Z, Yan H, Wang K, Kuang T, Zhang J, et al. 2004. Crystal structure of spinach major light-harvesting complex at 2.72 Å resolution. *Nature* 428(6980):287–92
121. Lunde C, Jensen PE, Haldrup A, Knoetzel J, Scheller HV. 2000. The PSI-H subunit of photosystem I is essential for state transitions in plant photosynthesis. *Nature* 408(6812):613–15
122. Makita Y, Suzuki S, Fushimi K, Shimada S, Suehisa A, et al. 2021. Identification of a dual orange/far-red and blue light photoreceptor from an oceanic green picoplankton. *Nat. Commun.* 12(1):3593
123. Mascoli V, Liguori N, Cupellini L, Elias E, Mennucci B, Croce R. 2021. Uncovering the interactions driving carotenoid binding in light-harvesting complexes. *Chem. Sci.* 12(14):5113–22
124. Meng EC, Goddard TD, Pettersen EF, Couch GS, Pearson ZJ, et al. 2023. UCSF ChimeraX: tools for structure building and analysis. *Protein Sci.* 32(11):e4792
125. Mishra RK, Ghanotakis DF. 1994. Selective extraction of CP 26 and CP 29 proteins without affecting the binding of the extrinsic proteins (33, 23 and 17 kDa) and the DCMU sensitivity of a Photosystem II core complex. *Photosynth. Res.* 42(1):37–42
126. Montané M-H, Kloppstech K. 2000. The family of light-harvesting-related proteins (LHCs, ELIPs, HLIPs): Was the harvesting of light their primary function? *Gene* 258(1):1–8
127. Mozzo M, Mantelli M, Passarini F, Caffarri S, Croce R, Bassi R. 2010. Functional analysis of Photosystem I light-harvesting complexes (Lhca) gene products of *Chlamydomonas reinhardtii*. *Biochim. Biophys. Acta* 1797(2):212–21
128. Myouga F, Takahashi K, Tanaka R, Nagata N, Kiss AZ, et al. 2018. Stable accumulation of photosystem II requires ONE-HELIX PROTEIN1 (OHP1) of the light harvesting-like family. *Plant Physiol.* 176(3):2277–91
129. Nagao R, Kato K, Hamaguchi T, Ueno Y, Tsuboshita N, et al. 2023. Structure of a monomeric photosystem I core associated with iron-stress-induced-A proteins from *Anabaena* sp. PCC 7120. *Nat. Commun.* 14(1):920
130. Nagao R, Kato K, Ifuku K, Suzuki T, Kumazawa M, et al. 2020. Structural basis for assembly and function of a diatom photosystem I-light-harvesting supercomplex. *Nat. Commun.* 11(1):2481
131. Nagao R, Kato K, Suzuki T, Ifuku K, Uchiyama I, et al. 2019. Structural basis for energy harvesting and dissipation in a diatom PSII-FCPII supercomplex. *Nat. Plants* 5:890–901
132. Naschberger A, Mosebach L, Tobiasson V, Kuhlgert S, Scholz M, et al. 2022. Algal photosystem I dimer and high-resolution model of PSI-plastocyanin complex. *Nat. Plants* 8:1191–201
133. Naumann B, Stauber EJ, Busch A, Sommer F, Hippler M. 2005. N-terminal processing of Lhca3 is a key step in remodeling of the photosystem I-light-harvesting complex under iron deficiency in *Chlamydomonas reinhardtii*. *J. Biol. Chem.* 280(21):20431–41
134. Nicol L, Croce R. 2021. The PsbS protein and low pH are necessary and sufficient to induce quenching in the light-harvesting complex of plants LHCII. *Sci. Rep.* 11(1):7415
135. Nicol L, Nawrocki WJ, Croce R. 2019. Disentangling the sites of non-photochemical quenching in vascular plants. *Nat. Plants* 5:1177–83
136. Niyogi KK, Björkman O, Grossman AR. 1997. Chlamydomonas xanthophyll cycle mutants identified by video imaging of chlorophyll fluorescence quenching. *Plant Cell* 9(8):1369–80

137. Niyogi KK, Björkman O, Grossman AR. 1997. The roles of specific xanthophylls in photoprotection. *PNAS* 94(25):14162–67
138. Niyogi KK, Grossman AR, Björkman O. 1998. Arabidopsis mutants define a central role for the xanthophyll cycle in the regulation of photosynthetic energy conversion. *Plant Cell* 10(7):1121–34
139. Nymark M, Valle KC, Hancke K, Winge P, Andresen K, et al. 2013. Molecular and photosynthetic responses to prolonged darkness and subsequent acclimation to re-illumination in the diatom *Phaeodactylum tricornutum*. *PLOS Biol.* 8(3):e58722
140. Ozawa S-I, Bald T, Onishi T, Xue H, Matsumura T, et al. 2018. Configuration of ten light-harvesting chlorophyll *a/b* complex I subunits in *Chlamydomonas reinhardtii* photosystem I. *Plant Physiol.* 178(2):583–95
141. Palm DM, Agostini A, Averesch V, Girr P, Werwie M, et al. 2018. Chlorophyll *a/b* binding-specificity in water-soluble chlorophyll protein. *Nat. Plants* 4:920–29
142. Pan X, Ma J, Su X, Cao P, Chang W, et al. 2018. Structure of the maize photosystem I supercomplex with light-harvesting complexes I and II. *Science* 360(6393):1109–13
143. Pan X, Tokutsu R, Li A, Takizawa K, Song C, et al. 2021. Structural basis of LhcbM5-mediated state transitions in green algae. *Nat. Plants* 7:1119–31
144. Park S, Fischer AL, Steen CJ, Iwai M, Morris JM, et al. 2018. Chlorophyll-carotenoid excitation energy transfer in high-light-exposed thylakoid membranes investigated by snapshot transient absorption spectroscopy. *J. Am. Chem. Soc.* 140(38):11965–73
145. Park S, Steen CJ, Lyska D, Fischer AL, Endelman B, et al. 2019. Chlorophyll–carotenoid excitation energy transfer and charge transfer in *Nannochloropsis oceanica* for the regulation of photosynthesis. *PNAS* 116(9):3385–90
146. Peers G, Truong TB, Ostendorf E, Busch A, Elrad D, et al. 2009. An ancient light-harvesting protein is critical for the regulation of algal photosynthesis. *Nature* 462(7272):518–21
147. Petrou K, Belgio E, Ruban AV. 2014. pH sensitivity of chlorophyll fluorescence quenching is determined by the detergent/protein ratio and the state of LHCII aggregation. *Biochim. Biophys. Acta* 1837(9):1533–39
148. Pi X, Tian L, Dai HE, Qin X, Cheng L, et al. 2018. Unique organization of photosystem I–light-harvesting supercomplex revealed by cryo-EM from a red alga. *PNAS* 115(17):4423–28
149. Pi X, Zhao S, Wang W, Liu D, Xu C, et al. 2019. The pigment-protein network of a diatom photosystem II–light-harvesting antenna supercomplex. *Science* 365(6452):eaax4406
150. Pinnola A, Alboresi A, Nosek L, Semchonok D, Rameez A, et al. 2018. A LHCB9-dependent photosystem I megacomplex induced under low light in *Physcomitrella patens*. *Nat. Plants* 4:910–19
151. Pinnola A, Cazzaniga S, Alboresi A, Nevo R, Levin-Zaidman S, et al. 2015. Light-harvesting complex stress-related proteins catalyze excess energy dissipation in both photosystems of *Physcomitrella patens*. *Plant Cell* 27(11):3213–27
152. Pinnola A, Dall'Osto L, Gerotto C, Morosinotto T, Bassi R, Alboresi A. 2013. Zeaxanthin binds to light-harvesting complex stress-related protein to enhance nonphotochemical quenching in *Physcomitrella patens*. *Plant Cell* 25(9):3519–34
153. Qin X, Pi X, Wang W, Han G, Zhu L, et al. 2019. Structure of a green algal photosystem I in complex with a large number of light-harvesting complex I subunits. *Nat. Plants* 5:263–72
154. Qin X, Suga M, Kuang T, Shen J-R. 2015. Structural basis for energy transfer pathways in the plant PSI-LHCI supercomplex. *Science* 348(6238):989–95
155. Rahmatpour N, Hauser DA, Nelson JM, Chen PY, Villarreal A JC, et al. 2021. A novel thylakoid-less isolate fills a billion-year gap in the evolution of Cyanobacteria. *Curr. Biol.* 31(13):2857–2867.e4
156. Rathbone HW, Michie KA, Landsberg MJ, Green BR, Curmi PMG. 2021. Scaffolding proteins guide the evolution of algal light harvesting antennas. *Nat. Commun.* 12(1):1890
157. Redekop P, Rothhausen N, Rothhausen N, Melzer M, Mosebach L, et al. 2020. PsbS contributes to photoprotection in *Chlamydomonas reinhardtii* independently of energy dissipation. *Biochim. Biophys. Acta Bioenerg.* 1861(5):148183
158. Röding A, Boekema E, Büchel C. 2018. The structure of FCPb, a light-harvesting complex in the diatom *Cyclotella meneghiniana*. *Photosynth. Res.* 135(1):203–11

159. Rossini S, Casazza AP, Engelmann ECM, Havaux M, Jennings RC, Soave C. 2006. Suppression of both ELIP1 and ELIP2 in Arabidopsis does not affect tolerance to photoinhibition and photooxidative stress. *Plant Physiol.* 141(4):1264–73
160. Ruban AV, Berera R, Ilioaia C, van Stokkum IHM, Kennis JTM, et al. 2007. Identification of a mechanism of photoprotective energy dissipation in higher plants. *Nature* 450(7169):575–78
161. Ruban AV, Saccon F. 2022. Chlorophyll *a* de-excitation pathways in the LHCII antenna. *J. Chem. Phys.* 156(7):070902
162. Ruban AV, Wentworth M, Yakushevska AE, Andersson J, Lee PJ, et al. 2003. Plants lacking the main light-harvesting complex retain photosystem II macro-organization. *Nature* 421(6923):648–52
163. Ruban AV, Young A, Horton P. 1994. Modulation of chlorophyll fluorescence quenching in isolated light harvesting complex of Photosystem II. *Biochim. Biophys. Acta Bioenerg.* 1186(1):123–27
164. Saccon F, Durchan M, Kaňa R, Prášil O, Ruban AV, Polívka T. 2019. Spectroscopic properties of violaxanthin and lutein triplet states in LHCII are independent of carotenoid composition. *J. Phys. Chem. B* 123(44):9312–20
165. Schaller S, Latowski D, Jemiola-Rzeminska M, Dawood A, Wilhelm C, et al. 2011. Regulation of LHCII aggregation by different thylakoid membrane lipids. *Biochim. Biophys. Acta* 1807(3):326–35
166. Schneider TD, Stephens RM. 1990. Sequence logos: a new way to display consensus sequences. *Nucleic Acids Res.* 18:6097–100
167. Scholes GD, Fleming GR, Olaya-Castro A, van Grondelle R. 2011. Lessons from nature about solar light harvesting. *Nat. Chem.* 3(10):763–74
168. Seiwert D, Witt H, Janshoff A, Paulsen H. 2017. The non-bilayer lipid MGDG stabilizes the major light-harvesting complex (LHCII) against unfolding. *Sci. Rep.* 7(1):5158
169. Seki S, Nakaniwa T, Castro-Hartmann P, Sader K, Kawamoto A, et al. 2022. Structural insights into blue-green light utilization by marine green algal light harvesting complex II at 2.78 Å. *BBA Adv.* 2:100064
170. Shen L, Huang Z, Chang S, Wang W, Wang J, et al. 2019. Structure of a $C_2S_2M_2N_2$-type PSII–LHCII supercomplex from the green alga *Chlamydomonas reinhardtii*. *PNAS* 116(42):21246–55
171. Shen L, Tang K, Wang W, Wang C, Wu H, et al. 2022. Architecture of the chloroplast PSI–NDH supercomplex in *Hordeum vulgare*. *Nature* 601(7894):649–54
172. Sheng X, Liu Z, Kim E, Minagawa J. 2021. Plant and algal PSII–LHCII supercomplexes: structure, evolution and energy transfer. *Plant Cell Physiol.* 62(7):1108–20
173. Sheng X, Watanabe A, Li A, Kim E, Song C, et al. 2019. Structural insight into light harvesting for photosystem II in green algae. *Nat. Plants* 5:1320–30
174. Shih PM, Wu D, Latifi A, Axen SD, Fewer DP, et al. 2013. Improving the coverage of the cyanobacterial phylum using diversity-driven genome sequencing. *PNAS* 110(3):1053–58
175. Shukla MK, Watanabe A, Wilson S, Giovagnetti V, Moustafa EI, et al. 2020. A novel method produces native light-harvesting complex II aggregates from the photosynthetic membrane revealing their role in nonphotochemical quenching. *J. Biol. Chem.* 295(51):17816–26
176. Simidjiev I, Stoylova S, Amenitsch H, Javorfi T, Mustardy L, et al. 2000. Self-assembly of large, ordered lamellae from non-bilayer lipids and integral membrane proteins in vitro. *PNAS* 97(4):1473–76
177. Skotnicová P, Staleva-Musto H, Kuznetsova V, Bína D, Konert MM, et al. 2021. Plant LHC-like proteins show robust folding and static non-photochemical quenching. *Nat. Commun.* 12(1):6890
178. Sobotka R, Tichy M, Wilde A, Hunter CN. 2011. Functional assignments for the carboxyl-terminal domains of the ferrochelatase from *Synechocystis* PCC 6803: The CAB domain plays a regulatory role, and region II is essential for catalysis. *Plant Physiol.* 155(4):1735–47
179. Staleva H, Komenda J, Shukla MK, Šlouf V, Kaňa R, et al. 2015. Mechanism of photoprotection in the cyanobacterial ancestor of plant antenna proteins. *Nat. Chem. Biol.* 11(4):287–91
180. Standfuss J, Terwisscha van Scheltinga AC, Lamborghini M, Kuhlbrandt W. 2005. Mechanisms of photoprotection and nonphotochemical quenching in pea light-harvesting complex at 2.5 Å resolution. *EMBO J.* 24(5):919–28
181. Stengel KF, Holdermann I, Cain P, Robinson C, Wild K, Sinning I. 2008. Structural basis for specific substrate recognition by the chloroplast signal recognition particle protein cpSRP43. *Science* 321(5886):253–56

182. Su X, Cao D, Pan X, Shi L, Liu Z, et al. 2022. Supramolecular assembly of chloroplast NADH dehydrogenase-like complex with photosystem I from *Arabidopsis thaliana*. *Mol. Plant* 15(3):454–67
183. Su X, Ma J, Pan X, Zhao X, Chang W, et al. 2019. Antenna arrangement and energy transfer pathways of a green algal photosystem-I–LHCI supercomplex. *Nat. Plants* 5:273–81
184. Su X, Ma J, Wei X, Cao P, Zhu D, et al. 2017. Structure and assembly mechanism of plant $C_2S_2M_2$-type PSII-LHCII supercomplex. *Science* 357(6353):815–20
185. Suga M, Ozawa S-I, Yoshida-Motomura K, Akita F, Miyazaki N, Takahashi Y. 2019. Structure of the green algal photosystem I supercomplex with a decameric light-harvesting complex I. *Nat. Plants* 5:626–36
186. Sun H, Shang H, Pan X, Li M. 2023. Structural insights into the assembly and energy transfer of the Lhcb9-dependent photosystem I from moss *Physcomitrium patens*. *Nat. Plants* 9:1347–58
187. Sundell D, Mannapperuma C, Netotea S, Delhomme N, Lin Y-C, et al. 2015. The plant genome integrative explorer resource: PlantGenIE.org. *New Phytol.* 208(4):1149–56
188. Swiatek M, Kuras R, Sokolenko A, Higgs D, Olive J, et al. 2001. The chloroplast gene *ycf9* encodes a photosystem II (PSII) core subunit, PsbZ, that participates in PSII supramolecular architecture. *Plant Cell* 13(6):1347–68
189. Swingley WD, Iwai M, Chen Y, Ozawa S, Takizawa K, et al. 2010. Characterization of photosystem I antenna proteins in the prasinophyte *Ostreococcus tauri*. *Biochim. Biophys. Acta* 1797(8):1458–64
190. Taddei L, Stella GR, Rogato A, Bailleul B, Fortunato AE, et al. 2016. Multisignal control of expression of the LHCX protein family in the marine diatom *Phaeodactylum tricornutum*. *J. Exp. Bot.* 67(13):3939–51
191. Takahashi H, Iwai M, Takahashi Y, Minagawa J. 2006. Identification of the mobile light-harvesting complex II polypeptides for state transitions in *Chlamydomonas reinhardtii*. *PNAS* 103(2):477–82
192. Takahashi K, Takabayashi A, Tanaka A, Tanaka R. 2014. Functional analysis of light-harvesting-like protein 3 (LIL3) and its light-harvesting chlorophyll-binding motif in *Arabidopsis*. *J. Biol. Chem.* 289(2):987–99
193. Tanaka R, Rothbart M, Oka S, Takabayashi A, Takahashi K, et al. 2010. LIL3, a light-harvesting-like protein, plays an essential role in chlorophyll and tocopherol biosynthesis. *PNAS* 107(38):16721–25
194. Thornber JP, Highkin HR. 1974. Composition of the photosynthetic apparatus of normal barley leaves and a mutant lacking chlorophyll *b*. *Eur. J. Biochem.* 41(1):109–16
195. Tian L, Nawrocki WJ, Liu X, Polukhina I, van Stokkum IHM, Croce R. 2019. pH dependence, kinetics and light-harvesting regulation of nonphotochemical quenching in *Chlamydomonas*. *PNAS* 116(17):8320–25
196. Tikkanen M, Mekala NR, Aro E-M. 2014. Photosystem II photoinhibition-repair cycle protects Photosystem I from irreversible damage. *Biochim. Biophys. Acta* 1837(1):210–15
197. Tikkanen M, Nurmi M, Suorsa M, Danielsson R, Mamedov F, et al. 2008. Phosphorylation-dependent regulation of excitation energy distribution between the two photosystems in higher plants. *Biochim. Biophys. Acta* 1777(5):425–32
198. Toporik H, Li J, Williams D, Chiu P-L, Mazor Y. 2019. The structure of the stress-induced photosystem I-IsiA antenna supercomplex. *Nat. Struct. Mol. Biol.* 26(6):443–49
199. Tsujimura M, Sugano M, Ishikita H, Saito K. 2023. Mechanism of absorption wavelength shift depending on the protonation state of the acrylate group in chlorophyll *c*. *J. Phys. Chem. B* 127(2):505–13
200. Tzvetkova-Chevolleau T, Franck F, Alawady AE, Dall'Osto L, Carrière F, et al. 2007. The light stress-induced protein ELIP2 is a regulator of chlorophyll synthesis in *Arabidopsis thaliana*. *Plant J.* 50(5):795–809
201. Varotto C, Pesaresi P, Jahns P, Leßnick A, Tizzano M, et al. 2002. Single and double knockouts of the genes for photosystem I subunits G, K, and H of Arabidopsis. Effects on photosystem I composition, photosynthetic electron flow, and state transitions. *Plant Physiol.* 129(2):616–24
202. Varsano T, Wolf SG, Pick U. 2006. A chlorophyll *a/b*-binding protein homolog that is induced by iron deficiency is associated with enlarged photosystem I units in the eucaryotic alga *Dunaliella salina*. *J. Biol. Chem.* 281(15):10305–15
203. Wang W, Yu L-J, Xu C, Tomizaki T, Zhao S, et al. 2019. Structural basis for blue-green light harvesting and energy dissipation in diatoms. *Science* 363(6427):eaav0365

194. Coined the term light-harvesting by differentiating the function between photosynthetic antenna proteins and reaction centers.

204. Wei X, Su X, Cao P, Liu X, Chang W, et al. 2016. Structure of spinach photosystem II-LHCII supercomplex at 3.2 Å resolution. *Nature* 534(7605):69–74
205. Wientjes E, Croce R. 2011. The light-harvesting complexes of higher-plant photosystem I: Lhca1/4 and Lhca2/3 form two red-emitting heterodimers. *Biochem. J.* 433(3):477–85
206. Wientjes E, Oostergetel GT, Jansson S, Boekema EJ, Croce R. 2009. The role of Lhca complexes in the supramolecular organization of higher plant photosystem I. *J. Biol. Chem.* 284(12):7803–10
207. Wientjes E, van Stokkum IH, van Amerongen H, Croce R. 2011. The role of the individual Lhcas in photosystem I excitation energy trapping. *Biophys. J.* 101(3):745–54
208. Wietrzynski W, Schaffer M, Tegunov D, Albert S, Kanazawa A, et al. 2020. Charting the native architecture of *Chlamydomonas* thylakoid membranes with single-molecule precision. *eLife* 9:e53740
209. Wolfe GR, Cunningham FX, Durnfordt D, Green BR, Gantt E. 1994. Evidence for a common origin of chloroplasts with light-harvesting complexes of different pigmentation. *Nature* 367(6463):566–68
210. Xiao Y, Huang G, You X, Zhu Q, Wang W, et al. 2021. Structural insights into cyanobacterial photosystem II intermediates associated with Psb28 and Tsl0063. *Nat. Plants* 7:1132–42
211. Xie H, Lyratzakis A, Khera R, Koutantou M, Welsch S, et al. 2023. Cryo-EM structure of the whole photosynthetic reaction center apparatus from the green sulfur bacterium *Chlorobaculum tepidum*. *PNAS* 120(5):e2216734120
212. Xu C, Pi X, Huang Y, Han G, Chen X, et al. 2020. Structural basis for energy transfer in a huge diatom PSI-FCPI supercomplex. *Nat. Commun.* 11(1):5081
213. Xu P, Tian L, Kloz M, Croce R. 2015. Molecular insights into zeaxanthin-dependent quenching in higher plants. *Sci. Rep.* 5(1):13679
214. Yakushevska AE, Keegstra W, Boekema EJ, Dekker JP, Andersson J, et al. 2003. The structure of photosystem II in *Arabidopsis*: localization of the CP26 and CP29 antenna complexes. *Biochemistry* 42(3):608–13
215. Yang D, Qing Y, Min C. 2010. Incorporation of the chlorophyll *d*-binding light-harvesting protein from *Acaryochloris marina* and its localization within the photosynthetic apparatus of *Synechocystis* sp. PCC6803. *Biochim. Biophys. Acta* 1797(2):204–11
216. Yeremenko N, Kouřil R, Ihalainen JA, D'Haene S, van Oosterwijk N, et al. 2004. Supramolecular organization and dual function of the IsiA chlorophyll-binding protein in cyanobacteria. *Biochemistry* 43(32):10308–13
217. Yokono M, Takabayashi A, Kishimoto J, Fujita T, Iwai M, et al. 2019. The PSI–PSII megacomplex in green plants. *Plant Cell Physiol.* 60(5):1098–108
218. Yoshihara A, Kobayashi K. 2022. Lipids in photosynthetic protein complexes in the thylakoid membrane of plants, algae, and cyanobacteria. *J. Exp. Bot.* 73(9):2735–50
219. You X, Zhang X, Cheng J, Xiao Y, Ma J, et al. 2023. In situ structure of the red algal phycobilisome–PSII–PSI–LHC megacomplex. *Nature* 616:199–206
220. Zabret J, Bohn S, Schuller SK, Arnolds O, Möller M, et al. 2021. Structural insights into photosystem II assembly. *Nat. Plants* 7:524–38
221. Zhang S, Tang K, Yan Q, Li X, Shen L, et al. 2023. Structural insights into a unique PSI–LHCI–LHCII–Lhcb9 supercomplex from moss *Physcomitrium patens*. *Nat. Plants* 9:832–46
222. Zhao L, Cheng D, Huang X, Chen M, Dall'Osto L, et al. 2017. A light harvesting complex-like protein in maintenance of photosynthetic components in *Chlamydomonas*. *Plant Physiol.* 174(4):2419–33
223. Zhao L-S, Wang P, Li K, Zhang Q-B, He F-Y, et al. 2023. Structural basis and evolution of the photosystem I–light-harvesting supercomplex of cryptophyte algae. *Plant Cell* 35(7):2449–63
224. Zhao S, Shen L, Li X, Tao Q, Li Z, et al. 2023. Structural insights into photosystem II supercomplex and trimeric FCP antennae of a centric diatom *Cyclotella meneghiniana*. *Nat. Commun.* 14(1):8164
225. Zheng L, Li Y, Li X, Zhong Q, Li N, et al. 2019. Structural and functional insights into the tetrameric photosystem I from heterocyst-forming cyanobacteria. *Nat. Plants* 5:1087–97
226. Zhou F, Liu S, Hu Z, Kuang T, Paulsen H, Yang C. 2009. Effect of monogalactosyldiacylglycerol on the interaction between photosystem II core complex and its antenna complexes in liposomes of thylakoid lipids. *Photosynth. Res.* 99(3):185–93